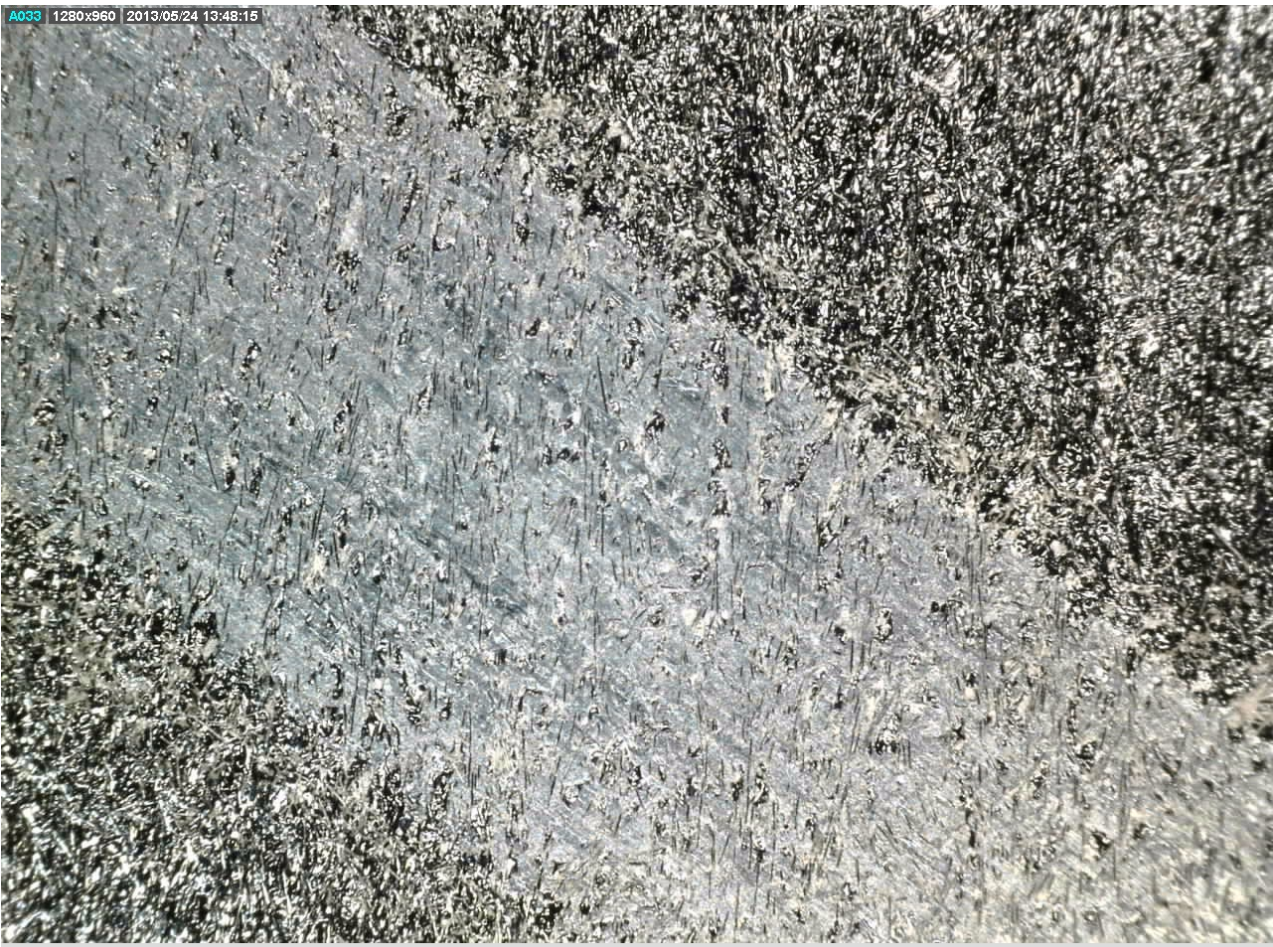


CHALMERS



Investigation of friction between plastic parts

Master's thesis in Polymer tribology

ERIK GUSTAFSSON

Department of Applied Mechanics

Division of Solid Mechanics

CHALMERS UNIVERSITY OF TECHNOLOGY

Göteborg, Sweden 2013

Master's thesis 2013:60

MASTER'S THESIS IN POLYMER TRIBOLOGY

Investigation of friction between plastic parts

ERIK GUSTAFSSON

Department of Applied Mechanics
Division of Solid Mechanics
CHALMERS UNIVERSITY OF TECHNOLOGY
Göteborg, Sweden 2013

Investigation of friction between plastic parts
ERIK GUSTAFSSON

© ERIK GUSTAFSSON, 2013

Master's thesis 2013:60
ISSN 1652-8557
Department of Applied Mechanics
Division of Solid Mechanics
Chalmers University of Technology
SE-412 96 Göteborg
Sweden
Telephone: +46 (0)31-772 1000

Cover:
Wear of one polymer from the friction and wear tests

Chalmers Reproservice
Göteborg, Sweden 2013

Investigation of friction between plastic parts
Master's thesis in Polymer tribology
ERIK GUSTAFSSON
Department of Applied Mechanics
Division of Solid Mechanics
Chalmers University of Technology

ABSTRACT

The goal for this master thesis is to improve and map the main factors behind friction and wear for a commercial product used by KONGSBERG AUTOMOTIVE. Components in a gear shifter are investigated and the target is to achieve high tribological quality of the force transmission. Finding a solution for low friction and wear which is independent of lubrication is the main issue for all involved components. Different material combinations, surface textures and load conditions are variables in this thesis.

Results presented are based on a literature, simulations, program development and tests. The objective for the literature study is to get knowledge about important factors which effects friction and wear for polymeric materials. Simulations is used for mapping constitutive variables in the contact region and analyze dependence of plasticity. A program written in MATLAB is developed for the FORCEBOARD (test equipment), where signals from transducers are processed and converted to static- and dynamic coefficient of frictions during long timespans. Reason for the program development is to achieve higher control in the experiments. Tests are performed with different material combinations, involved components are test plates and plungers similar to the actual application. Influence of textures are investigated for the material produced in purpose for low friction and high resistance against wear. The plunger is made of either one polymer type or steel. Time span for tests varies in purpose to compare the friction at initial state with the influence of wear. The equipment for the friction tests is a commercial product named FORCEBOARD. All tests are performed in a test rig with repeatable movements at KONGSBERG AUTOMOTIVES test laboratory.

Results show clear relation between friction and wear of polymeric materials used in the tests. Similar materials with different additives indicates large deviations for some tests. Experimental tests is the only reliable method for evaluating friction and influence by wear after large number of cycles. Results from conducted tests and related literature proved that both friction and wear are dependent on many variables e.g. contact pressure, temperature and surface topography. Test have also show that a suitable combination of materials and texture decrease the coefficient of friction and wear. Finally recommendations for further work are discussed.

Keywords: Tribology, Polymers , Wear, Low friction polymers, Contact simulations, Friction tests

PREFACE

First of all, i would like to thank my supervisor Kent Salomonsson at KONGSBERG AUTOMOTIVE for his deep knowledge in solid mechanics and never ending ideas which formed and developed this master thesis. At the same time, I want to thank my contact person Robert Fredriksson for his help and ideas during the work. I would also like to thank the remaining members of the simulation team at KA for their support and help. I dedicate my appreciation to Henrik Rudelius which made this master degree possible. The test- and prototype departments are also worth commendations for their support to establishment of a robust test set up. Finally, I would dedicate a a big thanks to Göran Brännare at Chalmers University of Technology for his interest and support for this master thesis.

Mullsjö, June 2013

Erik Gustafsson

NOMENCLATURE

Symbol	Description
v	Total specific volume of polymer
v_c	Specific volume of crystalline regions
v_a	Specific volume of amorphous regions
T_g	Glass transition temperature
T_m	Melting temperature
E	Youngs modulus
ν	Poisson ratio
E_r	Relaxation modulus
σ	Stress
ε	Strain
σ_y	Yield stress
ε_y	Yield strain
η	Viscosity in Kelvin model
σ_0	Constant tensile stress
α	Retardation time
V	Total volume of reinforcement material and matrix
V_f	Volume of glass fiber reinforced material
V_m	Volume of matrix material
ϕ_f	Portion of glass fiber reinforced material
ϕ_m	Portion of glass matrix material
E'	Combined Youngs modulus
R'	Combined radius
L	Length of cylinder for Hertzian theory
τ	Shear stress
p_0	Maximum normal stress
σ_{yy}	Normal stress
a	Contact radius
d	Deformation
F_N	Normal force
F_T	Tangential force
μ	Coefficient of friction
F_s	Static friction force
F_d	Dynamic friction force
a_i	Local contact area
f_i	Local vertical force
A_r	Area of real contact
H	Hardness parameter of the softer material
R_a	Arithmetic average
R_{max}	Maximum height of asperities
τ_y	Shear strength
F_p	Ploughing force
A_1	Load bearing area body 1
A_2	Load bearing area body 2
k	Wear coefficient

CONTENTS

Abstract	i
Preface	iii
Nomenclature	v
Contents	vii
1 Introduction	1
1.1 Background	1
1.2 Purpose	2
1.3 Limitations	2
2 Literature	4
2.1 Intro to polymeric materials	4
2.1.1 Basic of polymers	4
2.2 Mechanical properties of polymers	5
2.2.1 Creep	5
2.2.2 Stress relaxation	6
2.3 Glass fiber reinforcement	7
2.4 Test related polymers	8
2.5 Elastic contact	8
2.5.1 Elastic contact for cylinder-plane geometry	9
2.5.2 Elastic contact for sphere-plane geometry	9
2.6 Tribology	10
2.6.1 Intro tribology	10
2.6.2 Real area of contact	11
2.6.3 Surface topography	12
2.6.4 Adhesion and Deformation	12
2.6.5 Stick-Slip	13
2.6.6 Friction influence of normal load, velocity and temperature	14
2.6.7 Transfer film	15
2.6.8 Wear of polymers	15
2.6.9 Influence of glass fibre reinforcement	16
3 Method	17
3.1 Intro	17
3.2 Simulations	17
3.2.1 2D Elastic contact	18
3.2.2 3D Elastic contact	18
3.2.3 Stress-Strain behavior	19
3.3 Experimental tests	19
3.4 Test equipment	19
3.4.1 Matlab friction measurement	20
3.5 Test set up	21
3.6 Measurements	22
3.6.1 Influence of contact pressure	24
3.6.2 Texture tests	25

4 Results	26
4.1 Simulations	26
4.2 Experimental results	28
4.2.1 Material 30 minutes tests	29
4.2.2 Steel polymer test	33
4.2.3 900 minutes test	34
4.2.4 Friction dependence of normal load	36
4.2.5 Texture test	37
4.3 Wear	39
4.4 Summary of results	40
5 Conclusion and discussion	42
5.1 Conclusion	42
5.2 Sustainable development	43
5.3 Further work	43
6 Appendix	i
6.1 Appendix A	i
6.1.1 Texture figures	i
6.2 Appendix B	iv
6.3 Appendix C	v
6.4 Appendix D	vii
6.4.1 Texture figures	vii

1 Introduction

This section describe background, purpose and limitations of this master thesis.

1.1 Background

KONGSBERG AUTOMOTIVE provides world-class products to the global vehicle industry. Their main goals are to deliver products which enhance the driving experience, making it safer, more comfortable and sustainable. The company provides the automotive industry with a broad range of products worldwide. The products includes systems for seat comfort, clutch actuation, cable actuation, gear shifters, transmission control systems, stabilizing rods, couplings, electronic engine controls, specialty hoses, tubes and fittings. A large amount of products are produced in polymeric materials.

The application range of plastic parts in the automotive industry has grown since the introduction in the mid-1960s. The major reason using plastic parts instead of metal is less weight and simplicity producing complex geometries by injection molding. As new environmental decisions are made and taxes are formed, demands for reduce emissions can be fulfilled by replace metal against plastic parts. Most of the plastic parts are located in the interior but have lately been introduced in more mechanically loaded parts such as the engine. [14]

The tribological effects are important in the automotive applications since different parts are in contact with a large number of repetitive cycles e.g. the gear shifter. A combination of low friction and low wear is often desirable to obtain a high quality of a product throughout the lifetime. The friction and wear are often hard to predict from the material properties, in fact the combination of materials is more important. Therefore, it is usually necessary to carry out friction and wear tests for a specific application. During test conditions, it is important to imitate the actual conditions as much as possible, since many factors affect the friction and wear e.g. contact pressure, temperature and sliding velocity. Its also important to simplify tests by excluding unimportant variables. [9]

This thesis focuses on the tribological properties of a gearbox shifter see example in Figure 1.1. The aim of the application is to transmit power from the driver to the gearbox by a plunger slide against a track between different positions which corresponds to shifting in the car. There are various material options on both plunger and plunger track but usually low friction thermoplastics are utilized. The plunger track can be integrated in the shifter house with same material as the house or be added afterwards as an external material. The goal is to maintain as low friction as possible between the plunger and the plunger track. Low friction ensures self-seeking between gears and avoid end up midway between two gears in the shifter system.

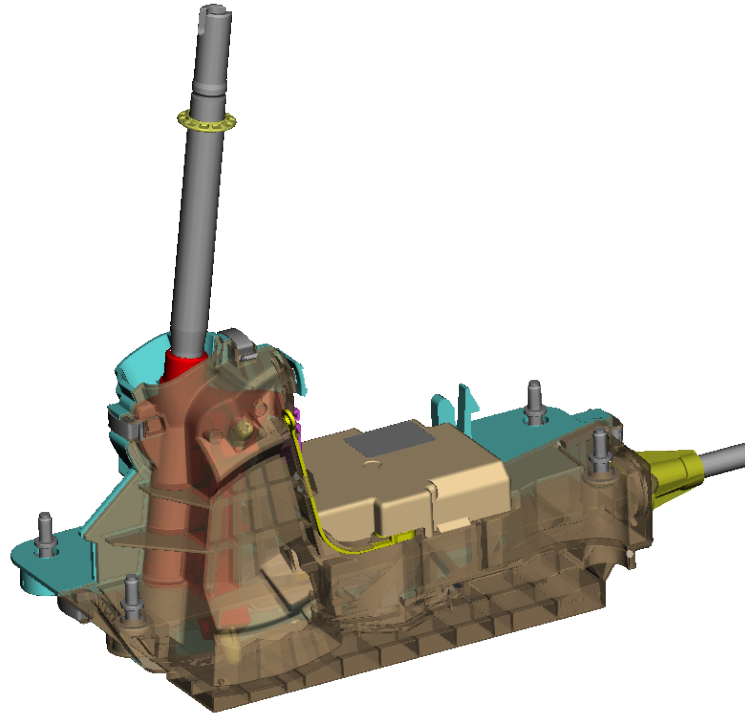


Figure 1.1: One model of a shifter house developed by KONGSBERG AUTOMOTIVE

1.2 Purpose

KONGSBERG AUTOMOTIVE have good knowledge in injection molded plastic parts. One important part in the pursuit of quality increase is knowledge and understanding about friction between moving plastic parts. The objectives of the thesis are:

- Analyze the underlying factors that influence friction between injection molded plastic parts.
- Investigate how friction is influenced by temperature changes.
- Investigate how friction is influenced by wear.
- Investigate effects of graining and structure for the frictional behavior.

The objectives are to improve a real product (gear shifter). Tests were performed with combination of different materials and the most important factors involved in the friction phenomena was isolated and tested in similar conditions. It exists a demand to perform materials tests with existing materials as well as some new proposed materials that has not previously used in production at KONGSBERG AUTOMOTIVE. There is also a request for examination of how different textures affect the friction. The main goal of the thesis is to find options which decrease friction to a level when lubrication can be omitted. A significant small wear is desirable to ensure low friction over high number of cycles that corresponds to the life span of a gear shifter.

1.3 Limitations

Limitations of this thesis have mainly focused on time and equipment. The friction is divided into static- and dynamic coefficient of friction, but dependency of the velocity is excluded in this work.

All measurements are performed at room temperature and no tests are conducted on either higher or lower temperatures. Measurements in a temperature chamber is difficult due to size of the test rig and the sensitivity of the measurement instruments. Maximum test duration is limited to 900 minutes, which corresponds to 9000 cycles and is significantly lower than the lifetime of the gear shifter which is estimated to 300000 cycles. The curvature of the plunger track is not considered in the tests due to limitations of the test equipment and number of influence variables. The plunger has an angle towards plunger track in reality but the orientation is always orthogonal against the test plates in this work. The plunger has a small hole located in the bottom that comes in contact with the track when the plunger is positioned without any incident angle. The hole is excluded in the finite element simulations for comparison with elastic theory which only handle simple geometries. This thesis does not address the influence of lubrication for friction and wear. No surface treatments are made on the materials, to avoid changes in the initial characteristics of the materials.

2 Literature

This section gives an introduction to relevant theory behind this master thesis. Purpose is to present the theory for important factors affecting friction and wear of polymeric materials. Even though the application targeting on low friction parts in gearbox shifters the main theory is valid for a wide range of applications.

2.1 Intro to polymeric materials

This section describe polymeric materials and their characteristics.

2.1.1 Basic of polymers

Polymers are build of carbon atoms connected by covalent bonds. Oxygen, Nitrogen and Hydrogen are common atoms connected to the carbon chains. Each repeatable unit is defined as monomer and the polymers are usually very long molecules with many repeatable units. Significant for polymers are high g/mol value. The molecules are connected to each other by secondary *Van der Waals*-, *dipole*- and *ion* bonds which are weaker than the intermolecular covalent bond. The mechanical properties of the polymer is characterized by the ability of movement in the molecule chains. Single bonds between carbon atoms causes a more ductile polymer compared to a double bonded. [15]

The processing of polymers is formed by addition of smaller monomers and this chemical process is named *polymerization* see Figure 2.1. If the polymer is build on one single monomer it's defined as *homopolymer* and if several monomers are involved the polymer is a *copolymer*. Since polymer chains are linked by *Van der Waals* bonds the strength increases for polymers with longer chains. The characteristics of a polymer are depending of the molecule chain structure. The structure for involved monomers and their's reactivity affect the final performance of the polymer. Most simple case are linear polymers build of one or more monomers in a linear chain. Branched chain could also be obtained in the *polymerization* process. A three dimensional cross linked structure can also be achieved in the creation process. Plastic materials are divided into different subcategories. [10]

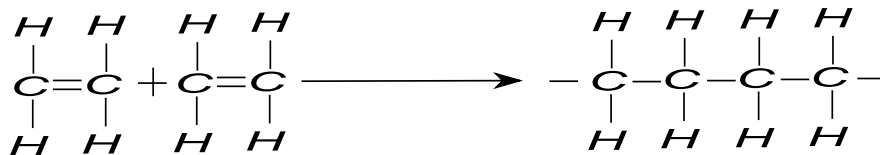


Figure 2.1: Polymer addition to part of polymer chain

- **Thermoplastics** - Build on linear or branched chains. The secondary bonds ends at moderate temperatures which increase the movement of the molecule chains and soften the material. At high temperatures over melting temperature T_m , the material transform to liquid phase. Many thermoplastics consists of two different regions which either are unordered or ordered. The unordered region has an amorphous structure and the ordered region has a crystalline structure.
- **Thermosets** - Are build on crosslinked polymer chains. The application design must be given initially since the thermosets can't melt and transform to liquid phase. Creation process includes additives which ease the formation of crosslinks within the polymer.

- **Elastomers** - Also known as rubber. Have cross linked polymer structure where molecules are able to move freely within the temperature range. Typically properties for this material are high elastic properties and rapid relaxation process.

A thermoplastics solid cant obtain full crystallization, but is a mixture of crystalline- and amorphous regions. The amount of each region is depending on temperature. By measuring specific volumes at room temperature (20°C) for crystalline region (v_c) and amorphous region (v_a) the specific volume for a specimen is calculated by (2.1).

$$v = xv_c + (1 - x)v_a \quad (2.1)$$

When the temperature for a polymeric material is decrease under the melting temperature T_m the crystallization begins. Nucleus starts to build below T_m and around each nuclei an spherulite starts to grow. The crystallization is finished when the spherulites grown so much that all space of the material is filled. During this phase amorphous regions are trapped between the crystal regions. [14] The semi crystalline polymers behaves as a mixture of both crystalline and amorphous phase. The amount of the crystalline phase could vary from 5-80%. The free volume increase significantly for the amorphous polymers at glass transition temperature T_g . This behavior is very significant for amorphous plastics and can also be observed for semi crystalline thermoplastics. [11] For semi-crystalline thermoplastics the strongest molecular bonds occurs in the crystalline regions. During initial plastic deformation the amorphous regions are stretched. Continued plastic deformation will divide the crystalline regions into even smaller regions which also might rotate depending on the load direction. [15]

Properties of polymeric material have a strong temperature dependence. The most critical temperatures are *glass transition temperature* T_g and *melting temperature* T_m . High temperatures below (T_m) tends to increase the ageing effects of the polymer. The *glass transition* temperature is when an amorphous region change properties from hard and brittle to a more rubber like behavior. The Young's modulus drops rapidly for amorphous thermoplastics over T_g . Therefore the application temperature should be less than T_g for an amorphous thermoplastic. For a semi crystalline thermoplastic the application temperature should preferable be larger than T_g but lower than T_m . Below T_g the material is brittle and when T_g is exceeded the semi crystalline material becomes hard and ductile. [10]

2.2 Mechanical properties of polymers

The deformation process for plastic materials involves elastic-, viscoelastic- and plastic characteristics, Figure 2.2 demonstrate this behavior for some material types. Plastic deformation occur for reasonable small loads, also temperature- and time dependence are significant for many polymers. The advantages with polymeric material is high mechanical strength relative to density. Figure 2.3a presents a typical case where a specimen exposed to a load which exceed the yield stress for the material. The load is removed after time t_0 , the strain relax back to zero after a certain time. This time dependency are very significant and important to include in calculations.

2.2.1 Creep

When a constant load is applied on a specimen over time a dependent deformation process called *creep* will take place. The deformation process is first elastic then time dependent viscoelastic. After a instantaneous load the creep rate is high until it reach a constant level. If the load is sufficient high the specimen will fracture after a certain time. [10] [11]. A typical creep behavior is displayed in Figure 2.3b

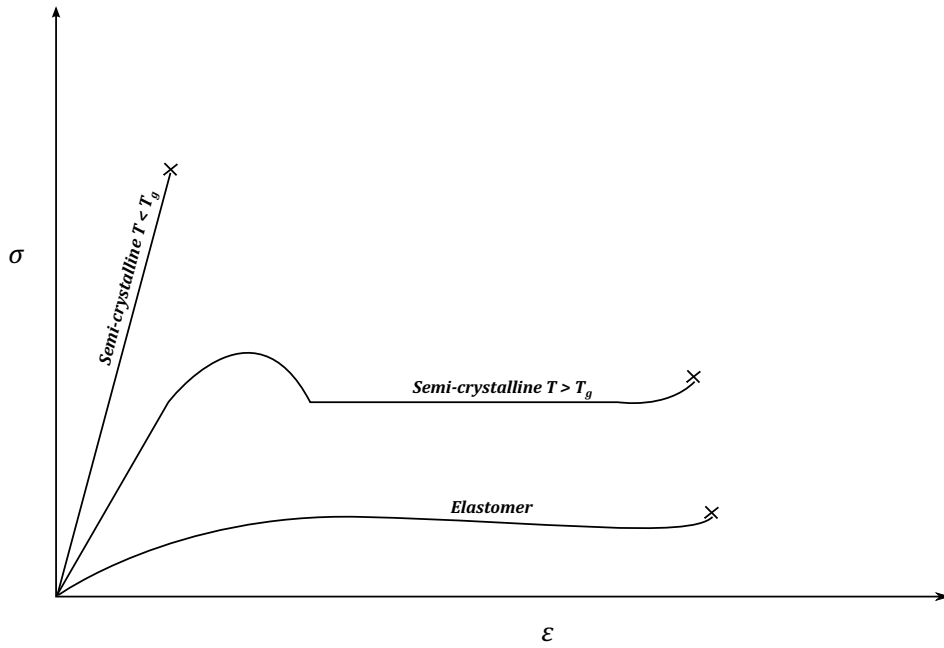


Figure 2.2: Typical deformation process for different polymers

2.2.2 Stress relaxation

For an ideal elastic solid the stress and strain is constant over time. For a linear viscoelastic solid the stress and strain instantaneously behaves in similar manner, but the stress will be reduced over time after reloading. An amorphous thermoset exhibits higher relaxation compared to a semicrystalline. The phenomena is named as *stress relaxation*. The relaxation dependence of Young’s modulus can be expressed by equation (2.2). [15] [11]

$$E_r(t) = \frac{\sigma(t)}{\epsilon} \tag{2.2}$$

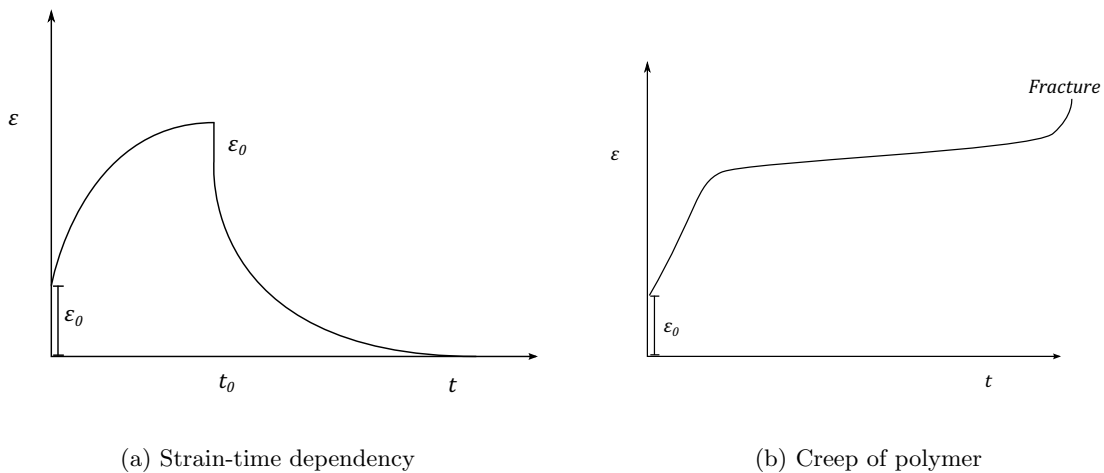


Figure 2.3: Time-dependent properties of polymers

Viscoelastic behavior is significant for polymeric materials. The definition of viscoelasticity is a

combination of elastic and viscous deformation characteristics. The elastic part of the deformation depends on stretching within the crystalline regions. The viscosity is created by diffusion of molecules in the amorphous regions. [12] The simplest material description of viscoelastic time dependent deformation is the Kelvin model. The model is a linear spring parallel connected with a damper, where the elastic part is modeled with the spring ($\sigma_1 = E\varepsilon$) and the viscous part ($\sigma_2 = \eta \frac{d\varepsilon}{dt}$) with the damper see Figure 2.4.

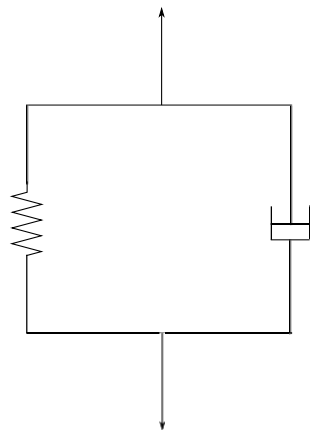


Figure 2.4: The Kelvin model

The stress and strain for the Kelvin model are expressed by the equation (2.3) and (2.4).

$$\sigma = \sigma_1 + \sigma_2 = E\varepsilon + \eta \frac{d\varepsilon}{dt} \quad (2.3)$$

$$\varepsilon = \varepsilon_1 = \varepsilon_2 \quad (2.4)$$

The solution of the first order differential equation is

$$\varepsilon(t) = \frac{\sigma_0}{E} \left(1 - e^{-t/\alpha} \right) \quad (2.5)$$

Equation (2.5) describe the time dependent deformation at constant loading. The strain $\frac{\sigma_0}{E}$ represent the deformation after a long time and $\alpha = \frac{\eta}{E}$ describe the material time dependence. The Kelvin model can not present a material with stress relaxation. Another model named Maxwell is serial connection between a spring and a damper. This model has full stress relaxation properties and is used for presenting liquids under short time load. The easiest deformation model for polymers are the Burger model which is a combination of Maxwell and Kelvin. [10]

2.3 Glass fiber reinforcement

Common method to improve the mechanical properties or performance at wide temperature range is to include a glass fiber reinforcement in the polymer. Reinforcement material shall have characteristics which increase the stiffness and ability to tie well to the matrix. Glass fiber is the most common reinforcing material for an application at low price. The proportion of volume fraction of reinforcing material and the matrix is defined by the equation (2.6)

$$V = V_f + V_m \quad (2.6)$$

The total amount of fiber is defined as $\phi_f = \frac{V_f}{V}$ and amount of matrix $\phi_m = \frac{V_m}{V}$. The diameter of glass fibers are in the range 5-15 μm . Typical length of short glass fibers is 0.2-0.5 mm and for

long glass fibers 4-10 mm. For injection molded short fiber plastic its often common with a random distribution of the glass fiber within the structure.

2.4 Test related polymers

The polymers utilized for experiments in this thesis are variations of Polyamides (PA) and Polyoxymethylene (POM). This section cover some basic facts about these polymers. Both polymers are suitable for injection molding.

Polyamide

PA is a semi-crystalline thermoplastic and the molecular formula is presented in Figure 2.5a. There are several variants of such as PA6, PA66 and PA46. The number refers to the molecule structure of the polymer which determine the properties, e.g. PA46 contain aromatics in the molecule chain which enable higher application temperatures. Generally PA have good combination of mechanical- and chemical properties. Other favorable characteristics are high tolerance against creep, fatigue and abrasion. This polymer is suitable for glass fiber reinforcement to enhance the mechanical properties [10]

Polyoxymethylene

POM is a high crystalline thermoplastic with a wide range in application temperature and applications. The molecular formula of is displayed in Figure 2.5b. POM is ductile in combination with high toughness. Good resistance against stress relaxation and thermal degradation. Generally known for excellent tribological properties. [10]

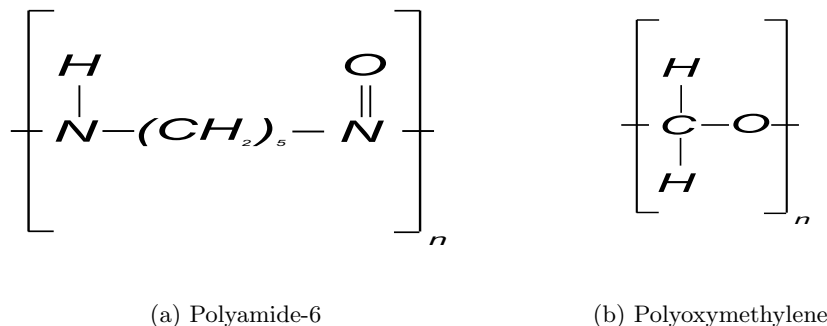


Figure 2.5: Molecular formulas

2.5 Elastic contact

Friction between bodies results in energy dissipation. In reality the contact area is hard to predict and is usually smaller than expected. Materials are often exposed for high stresses in the contact region with wear as resulting in microscale fatigue. In many cases it is sufficient to use the theory of elastic contact to evaluate contact area and deformation of solids. The main assumptions for this Hertzian theory are: [7]

- The material behaves linear elastic at all stresses and strains

- The theory treats ideal smooth surfaces.
- Frictional free contact between the bodies.
- Contact area is small compared to the curvatures of the bodies.
- Max pressure is obtained in the center of the contact and decrease quadratically.

The theory can handle different load cases and the two dimensional case represent a cylinder in contact with an infinitely elastic plane. The three dimensional case represent a sphere against an infinitely elastic plane. For both cases a combined Young modulus and radius for the bodies is calculated by equations (2.7)-(2.8).

$$\frac{1}{E'} = \frac{1 - \nu_1^2}{E_1} + \frac{1 - \nu_2^2}{E_2} \quad (2.7)$$

$$\frac{1}{R'} = \frac{1}{R_1} + \frac{1}{R_2} \quad (2.8)$$

Where $R_2 \rightarrow \infty$ since body two represent a plane.

2.5.1 Elastic contact for cylinder-plane geometry

Equations (2.9)-(2.12) are used to calculate the maximum normal- and shear stress and contact radius for the case with cylinder against a plane.

$$p_0 = -0.564 \left(\frac{F_N E'}{L R'} \right)^{1/2} \quad (2.9)$$

Where p_0 is equivalent with the normal stress and used to obtain the value for maximal shear stress. L represent the length of the model in plane.

$$\tau_{max} = 0.3p_0 \quad (2.10)$$

The deformation is obtained for the relation between normal stress and combined Young's modulus.

$$d = \frac{4F_N}{\pi E'} \quad (2.11)$$

The contact radius is obtained for relation between combined radius and deformation.

$$a = \sqrt{R' d} \quad (2.12)$$

2.5.2 Elastic contact for sphere-plane geometry

Equations (2.13)-(2.15) are used to calculate the maximum normal-, shear stress and deformation for the case with a sphere against a plane.

$$p_0 = -0.578 \left(\frac{F_N E'^2}{L R'^2} \right)^{1/3} \quad (2.13)$$

$$\tau_{max} = 0.31p_0 \quad (2.14)$$

$$a = \frac{\pi p_0 R'}{2E'} \quad (2.15)$$

$$d = \frac{a^2}{R'} \quad (2.16)$$

This theory results in knowledge about the contact area and stresses obtained in the experiments and finite element calculations. [7] [1] [18]

2.6 Tribology

2.6.1 Intro tribology

Tribology is defined as the science of bodies in relative motion and involves friction, wear and lubrication. [7]. Tribology has been studied for over centuries and early observations defined the coefficient of friction as (2.17).

$$\mu = \frac{F_T}{F_N} \quad (2.17)$$

Where F_T represent the tangential force and F_N the normal force.

In reality it's hard to predict the friction and wear between bodies from material parameters and geometry. Most of materials have the ability to change their characteristics under friction and wear. The material may deform and be exposed for chemically reactions in the local connection spots. There are many parameters which are important for a tribosystem to avoid radical changes in the wear and friction over time. [7]

From experimental results Coulomb observed in the 1700 century that friction force to overcome movement of a body was proportional to the normal load. This critical force was defined as (2.18). Coulomb found this force to be independent of contact area and the roughness of the surface.

$$F_s = \mu_s F_N \quad (2.18)$$

The dynamic friction coefficient was defined from observation when the body has transferred to stable movement. Coulomb also found this force proportional to the normal load as (2.19). The value of the dynamic friction coefficient was found to be equal to the static coefficient or smaller.

$$F_d = \mu_d F_N \quad (2.19)$$

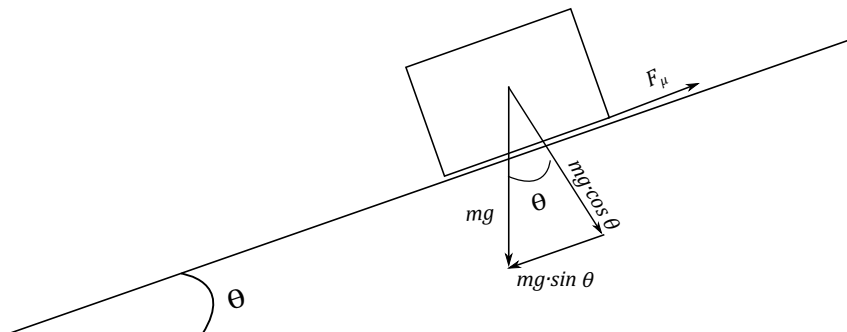


Figure 2.6: The leaning plane for equilibrium equation (2.20)

The most simple case of friction is a leaning plane shown in Figure 2.6. From the free body diagram the coefficient of friction can be obtained to overcome the static friction. The value of μ_s can be

estimated with a Dynamometer. Equation (2.20) represent the expression for the static coefficient of friction from the free body diagram of the mass on leaning plane. [18]

$$\mu_s = \frac{F_T}{F_N} = \frac{mg\sin(\theta)}{mg\cos(\theta)} = \tan(\theta) \quad (2.20)$$

The theory behind tribology for solids are applicable for many types of material. Polymers fits to represent the general case even though there are a lot of differences between polymers and metals. [2]

2.6.2 Real area of contact

Since no surface are ideally flat it's hard to predict the *real area of contact*. The real area of contact refers to the sum of local contact points that come in contact when the bodies are brought together see Figure 2.7. Asperities from the two bodies deforms elastic or plastic to contact spots until the area is sufficiently large to carry the normal load. All the local connection spots represent the real area of contact and can be expressed by (2.21) . The asperities occur from deviations on microlevel. At the same manner can the normal force be expressed as a sum of vertical forces for in each local contact spot by equation (2.22)

$$A_r = \sum_{i=1}^n a_i \quad (2.21)$$

$$F_N = \sum_{i=1}^n f_i \quad (2.22)$$

It's difficult to predict the real area of contact without any deeper knowledge about surface topography and material parameters. A good approximation can be used to estimate the contact area on each spot or for the entire geometry. The expressions is obtained from the relation between the normal force and hardness parameters for the softer material as equations (2.23)-(2.24).

$$a_i = \frac{f_i}{H} \quad (2.23)$$

$$A_r = \frac{F_N}{H} \quad (2.24)$$

Where H represent the hardness parameter for the softer material. From equation (2.23)-(2.24) it's clear that the contact area are proportional to the normal load and independent of the surface topography. [7]

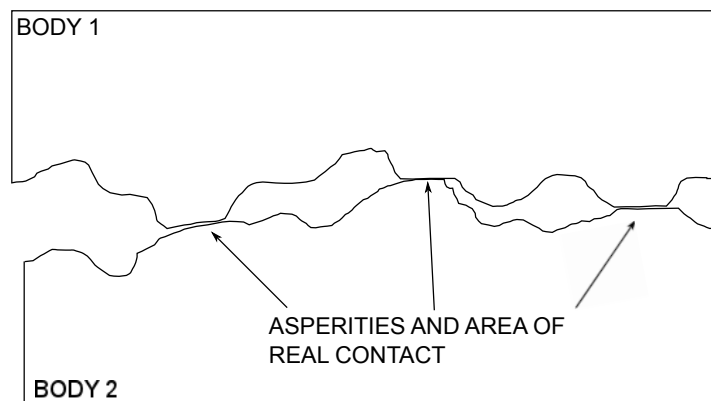


Figure 2.7: Asperities and area of real contact

2.6.3 Surface topography

As previously mentioned no surface can be perfectly smooth. There are always some deviation of the surface that can be from the range of impurities on atomic scale to deviations from production process. The most common way to reduce roughness on a surface is to polish it. The deviations on a surface can be subdivided into different categories:

- **Macro deviations** - Occurs from deviations and lack of stiffness in the tool at the machining process.
- **Roughness** - Deviations from vibration- waviness- and wear from the tool in the machining process
- **Micro roughness** - From imperfections in material at atomic scale and non uniform deformation at the surface.

The micro roughness known as asperities and is one of the main factors behind sliding friction. Asperities are important for the friction due to they determine the contact between bodies. Since there may exist a high number of asperities on a surface it can be difficult to determine the surface characteristics. The most common way to measure a surface asperities is by use of Profilometer with a tip radius of 2 micrometer or less. The vertical asperities are measured by moving the tip over the surface and the signal is amplified. The most common method to evaluate the surface roughness is to calculate the R_a and RMS value. The R_a value represent the mean vertical deviation from the centerline and is calculated by equation (2.25)

$$R_a = \frac{1}{L} \int_0^L |z(x)| dx \quad (2.25)$$

For bodies in contact only the upper tops of the asperities are involved at the beginning of the contact but this changes dramatically when the surface begins to slide relative to each other. [6] If a smooth surface is desirable the most common way is to polish the surface to make it more uniform. Under the polish process the material are exposed for high shear stresses and a hard smooth layer is created at the surface. The polish process tends to change the characteristics of the materials at the surface regions.[7]

2.6.4 Adhesion and Deformation

The main tribological properties contributing to friction are adhesion and deformation. Adhesion refers to the shearing at local contact spots. Adhesive bonds exists in the contact region for polymers. Molecular bonds are created between contact surfaces in the same manner as within the polymers. The strength of the bond between the surfaces can be almost as strong as within the bulk polymer. Therefore under sliding condition elements of one polymer surface can be torn away from the opposite surface. The deformation component in tangential direction refers to the sliding over the asperities of the surfaces. The deformation can be compared with plowing, where tangential force must be great enough to pass over the asperities while surfaces might slide or shear depending on relative mechanical properties. To avoid strong adhesive forces between polymers a lubrication can be utilized. [8]

Adhesion component

The adhesion component of the friction can be explained by the following process: When a tangential force is applied it first results in sliding on microscale causing elastic deformation of the asperities.

Contact spots breaks when the pressure exceed the shear strength τ_y of the softer material. The friction force is caused by shearing of the connection spots and therefore low adhesion forces between bodies are desirable. During the sliding process new connection spots are produced and high shearing deformation and fatigue of local connection spots between the bodies are continuous. The tangential force can be expressed as combination of the shear strength and the area of real contact by equation (2.26).

$$F_T = \tau_y A_r \quad (2.26)$$

Combining equations (2.17), (2.24) and (2.26) an analytical expression for the coefficient is obtained by the equation (2.27)

$$\mu = \frac{\tau_y}{H} \quad (2.27)$$

The equation (2.27) clarify that the coefficient of friction is dependent of material parameters for the softest material. It also explain independence of contact area, sliding velocity, contact pressure and surface topography. This theory is very generalized and there are many materials that deviate from this behavior, especially polymers. [7]

In reality adhesion between surfaces are related to the contact pressure at actual temperature. For higher temperatures and pressures the adhesive bonds between polymers tends to increase and more plastic deformation is involved when bodies are brought together. The bonds between bodies are mainly of *Van der Waals* type, but also hydrogen bonds can arise if the distance between bodies are sufficiently small. The adhesive component is believed to be the major contribution to the friction compared to the deformation component [9]

In reality the relative hardness and temperature softening for the material is also very prone to affect the friction. The friction often increase between equal polymers compared to two different polymers. The reason for this behavior is presence of high molecular adhesion which is significant for high friction. [11]

Deformation component

For very smooth surfaces the friction law in equation (2.27) can be considered valid for some materials. In cases with more rough surfaces the force contribution caused by plowing through the softer material asperities affects the friction significantly. For rough surfaces an additional term is added to the coefficient of friction which take care of the plowing term. The plowing forces can be related to the hardness of the softer material in the same manner as the normal force in equation (2.24). The expression for the deformation component can be expressed by equation (2.28). The total expression for the coefficient of friction is now expressed by $\mu = \mu_{\text{adhesion}} + \mu_{\text{deformation}}$. [7]

$$\mu_{\text{deformation}} = \frac{F_P}{F_N} = \frac{A_1 H}{A_2 H} = \frac{A_1}{A_2} \quad (2.28)$$

The deformation component arise from asperities from plough tracks created by the harder material. Since the hardness for polymers is less than most of the metals the deformation component is very important for abrasive wear on polymer surfaces. [11]

2.6.5 Stick-Slip

From experiment the friction in most cases won't show a continuous process. The stick-slip motion results from conditions where static friction is higher than the dynamic and occur for very small velocities. The stick process happens when the contact area increases and the slip process occur when

the tangential force is sufficiently high to shear the junctions and plough the material. The coefficient of friction and area of contact are high during the stick and decrease rapidly during the slip process. [11]

When two surfaces moves jerkily against each other as under the stick-slip motion a grinding noise might be created. Junctions are created and ceases in a discontinuous motion and cause this sound. The criteria for the stick-slip motion phenomena are:

- The static friction coefficient should be greater than the dynamic.
- There exists some elastic deformation in the contact.

The stick-slip motion can be decreased by reducing the normal load or increase the sliding velocity. [7] Typical friction force behavior for stick-slip motion phenomena is displayed in Figure 2.8

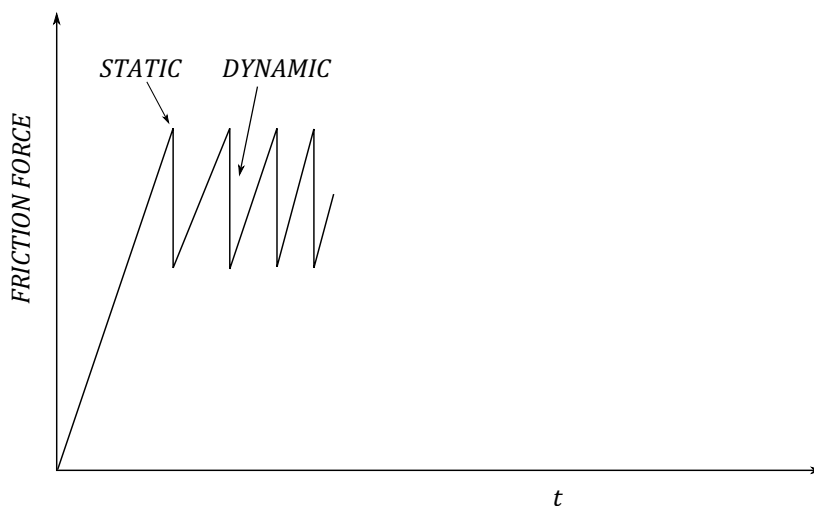


Figure 2.8: Stick-slip of friction for and time

2.6.6 Friction influence of normal load, velocity and temperature

Theoretical by equation (2.18)-(2.19) the coefficient of friction is proportional to the normal load. This criteria is just fulfilled for some polymers under specific conditions. Many experiments have been performed with variable normal loads. There is difficulties to generalize the results since it differs from polymer to polymer, the result might be that friction is constant or decrease/increase by the normal load. This behavior depends on size of initial asperities, wear and material properties. For example a certain normal load the friction start to increase and this is depending of transition from elastic to plastic deformation of the asperities. After a while the asperities are reduced due to contact with a harder surface and this may decrease the coefficient of friction[9].

In the same manner as the normal load the coefficient of friction shall be independent of the sliding velocity. In reality the coefficient have a tendency to vary with the sliding velocity. The velocity dependent is hard to predict but its related to a micro scale process for the bodies in contact. General the velocity dependent can be considered as stable for temperatures less than T_g . For normal temperatures it's difficult to predict the velocity influence because it is depending of visco-elastic behavior of the polymer. At low velocities the viscous resistance increase for ascending velocities, but for higher velocities the elastic deformation in the contact spots are most pronounced and then the

velocity dependence decrease against a stable value. [9] Measurements at different velocities are the only practical method for observations of this dependency.

Since the polymers behaves visco-elastic they are sensitive to heating during the friction process. The frictional heating is created in the spots of real contact between bodies. The formation and break up of adhesive bonds are affected by temperature and therefore also the coefficient of friction. Tests has been performed for different material combinations and temperatures, the coefficient showed tendency to both increase and decrease for different material combinations. In a generalized sense the temperature dependence increases at temperatures above T_g . [9]

2.6.7 Transfer film

When a material slides against a polymer a transfer film is developed from rupture within the polymer and adhere to the opposite counter face. This happens for most of the polymers except the highly cross linked and some glassy polymers.[2] From the adhesion between the polymers the formation of the transfer film is important for tribological aspects. From the experiments of steel-tribo system it has been established that the transfer film from polymers have a tendency to adhere on metal surfaces and in turn influence on friction and wear. [9]

The wear rate of the polymers have shown to be significantly affected by the formation of the transfer film. From observation of a steel- and polymer tribo system its been found that the fragments of the polymer were found in the asperities of the steel face. Before and after formation of the transfer film the friction is dependent of the initially and changed deformation properties of the polymer. The loss and formation of the transfer films is explained to the adhesive bonds. [16] The wear of polymers from the transfer film changes the topography of the counter face and at the same time affect the wear rate. [5]

2.6.8 Wear of polymers

For tribological contacts the initial conditions changes over time, this can involve changes in the geometry, topography, the microstructure and composition of the material. There are different wear types involved and usually it's not just a wear type that exists but rather a combination of several. In most cases the wear is undesirable and affects the life-span and friction negatively. There are a variety of parameters which control the wear of various materials, some of these are the contact pressure, temperature, and sliding velocity. [7] Wear types for polymers are mainly adhesion, abrasion and fatigue. The wear of polymers is a complex process which clearly is related to the formation of the transfer film. Chemical reactions occur in the contact spots which makes it hard to predict the wear. Additives in the polymer composition have also an effect on the tribological behavior. [9]

Abrasive wear is defined as wear by displacement of material through relative motion between the surfaces. This wear occur from hard asperities from one of the material or can also derive from hard particle embedded in one of the materials. The wear can be subdivided into two body abrasion and three body abrasion, where three body abrasion involves hard particle in the tribo system. For the two body abrasion the asperities from the hard material plough the surface of the softer material, and the wear rate is dependent on the shape of the asperities. [5] Experimental correlation have been established for the abrasive wear. The wear rate of polymers was found to be related to the yield stress- and strain of the softer material as described in equation (2.29)

$$k \propto \frac{1}{\sigma_y \varepsilon_y} \quad (2.29)$$

Equation (2.29) explain that the wear rate is proportional to the inverse of the double strain energy for the softer material. Abrasive wear between two body is usually a combination of ploughing and micro cutting of small chips from the material. [9]

The adhesive wear of polymers relates to the formation, shearing and rupture of the adhesive junction in the contact spots. Material transfer from one surfaces to another can drastically change wear rate. When the transfer film from the polymer is continuously created and smeared out the wear rate increases. For some combination of materials the thickness of the transfer film grows towards an asymptotic value. From loss of material from the softer polymer roughness of the surface can vary a lot until the steady wear rate is reached. [9]

Fatigue wear arise from repeated cyclic stresses in the material. The crack propagation start at the point with highest tangential stress or tensile strain. The fatigue wear only involves the region close to the surface. An correlation have been found for $\mu < 0.3$ the maximum shear stress is located below the surface and for higher friction coefficient values its located closer to the surface. [9]

2.6.9 Influence of glass fibre reinforcement

From experiments it has been shown that the reinforcement material can have a positive effect on friction but particularly for the combination of reinforced polymers and steel. Reinforcement increases the strength of the material which in turn reduces wear dramatically. The best reinforcement material is carbon fiber with lubricating properties, but also glass fiber has similar characteristics of the wear rate. Although steel is usually much harder than the glass fiber a small wear has been observed on steel surfaces. There is lack of documentation for polymer against polymer with reinforced glass fiber and documented cases mostly refer to very specific polymer combinations under specific conditions. [17]

3 Method

This section presents the workflow for the thesis.

3.1 Intro

The work is divided into experimental tests and simulations. For the simulations, mainly contact phenomena have been of interest. Theoretical values are compared with numerical obtained by Finite Element Analysis (FEA). Experimental tests focused on evaluating the static- and dynamic friction for polyamide and steel against different combinations of polymers. The evaluated material in this thesis involves:

- Different variations of POM with low friction additives.
- Two types of polyamides.
- One glass fiber reinforced polyamide.
- One ABS resin with 14 different surface textures.

Simulations and tests are performed on plunger and plunger track which are subcomponents in a gearshift system, see Figure 3.1.

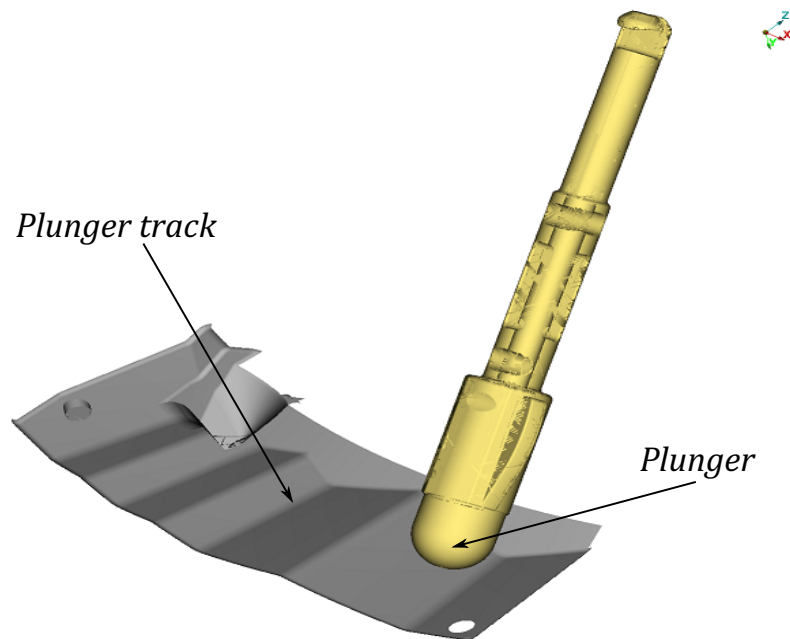


Figure 3.1: Plunger and belonging plunger track for one of KA models

3.2 Simulations

For all simulations ANSA, LS-DYNA and META are used as pre-processor, solver and post-processor. The models resembled a sphere and cylinder against an infinitely elastic plane. Since this isn't realistic in a FE-model, boundary conditions are used to dissemble that behavior. Theoretical values for

the Hertz contact stress and the contact area are calculated in MATLAB, explained in Section(2.5). The implicit solver is utilized for all simulations. Since KONGSBERG AUTOMOTIVE have excellent computational resources a fine mesh is possible for simulations. Simulations is performed with both linear elastic (1)- and piecewise linear plasticity (24) material properties. [4] The normal load is ramped from 0 to 100 N during one second for all simulations.

3.2.1 2D Elastic contact

For the two dimensional case the contact zone is modeled with outer contour similar to the plunger. The model is presented in Figure 3.2a. Constant strain triangle elements are implemented in the model with the thickness of one unit length perpendicular to the plane. Simulation materials with their respective geometry are presented in Table 3.1. The load are equally distributed on nodes at the upper boundary in the vertical direction. To avoid overlapping of element in the contact zone, the penalty factor for the contact algorithm is increased by a factor of ten. This was found by testing different values and penalty factor equal to ten avoid overlapping of elements. The model is refined in the contact spots since initially only a small number of element are in contact before deformation. A fine mesh results in convergence of the stresses in the contact zone. The lower boundary conditions for the plane are fixed for all translations and rotations. The upper body is constrained for all rotations to avoid tilt.

Table 3.1: Material properties for 2D and 3D simulations

Part	E [MPa]	ν	ρ $[\frac{kg}{m^3}]$	r [mm]
Plunger (PA)	1000	0.35	1180	4
Plane (POM)	2870	0.35	1410	-

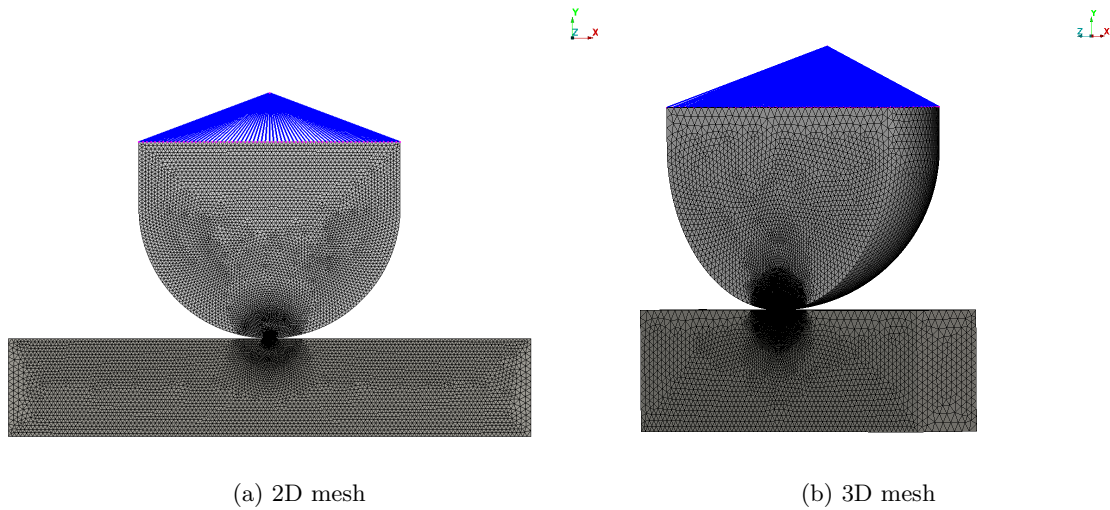


Figure 3.2: FE models for simulations

3.2.2 3D Elastic contact

The 3D-model is implemented with tetrahedron elements and refined in the contact zone, this required large number of elements. Since the plunger is rotational symmetric a symmetry boundary condition is utilized to reduce the computational time. Simulation models are displayed in Figure 3.2b.

3.2.3 Stress-Strain behavior

The normal stress, shear stress and deformation are also calculated with material properties describing plasticity. The stress strain curve for the PA and POM are displayed in Figure 3.3. Purpose of these simulations is to capture the real behavior of the polymers and compare with theoretical values and pure elastic material properties.

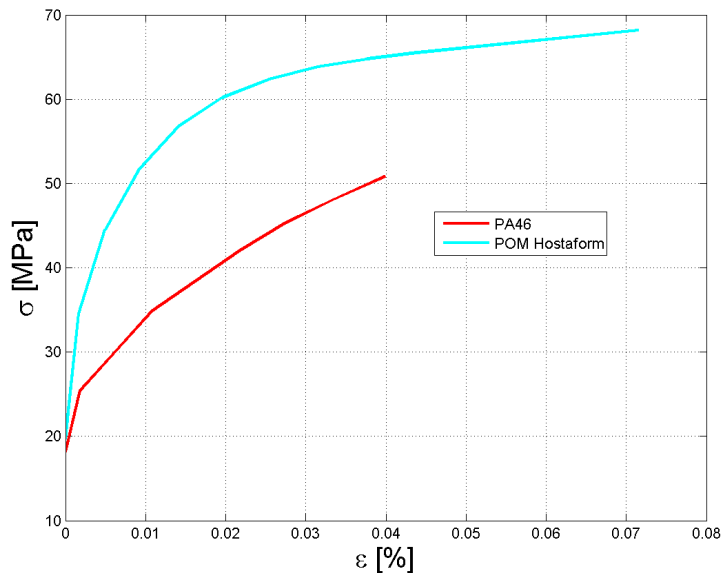


Figure 3.3: Stress-Strain curves used for simulation(PA and POM)

3.3 Experimental tests

All tests are performed at KONGSBERG AUTOMOTIVES test laboratory. The application is exposed to a high number of cycles over a lifetime and friction conditions may change due to the influence of wear, see Section 2.6.8. Therefore conducted tests are performed from 30- to 900 minutes for evaluation of wear. The materials used for tests was selected by one of the the plastic supplier for KONGSBERG AUTOMOTIVE. Requirements of produced resins are characteristics for low coefficient of friction and high resistance against wear. Produced test plates were injection molded at KONGSBERG AUTOMOTIVE and patterned with different surface textures. Material tests are conducted for three different distinguished textures for analyzing the relation between surface finish and coefficient of friction.

3.4 Test equipment

The equipment used for measuring friction is the FORCEBOARD, see Figure 3.4 which contains strain gauge transducers in horizontal and vertical direction. This FORCEBOARD is delivered with a software for measure and storing data. The FORCEBOARD is limited to a tangential force at 30N and normal force at 100N, therefore experiments are adjusted to those limitations. The software delivered for the FORCEBOARD is also limited to a sampling frequency of 50 Hertz. Therefore a new program is developed in MATLAB for controlling and evaluating measured data, see section 3.4.1. The developed software made it possible to sample data at higher frequencies than 50 Hz to capture and resolve static coefficient of friction.

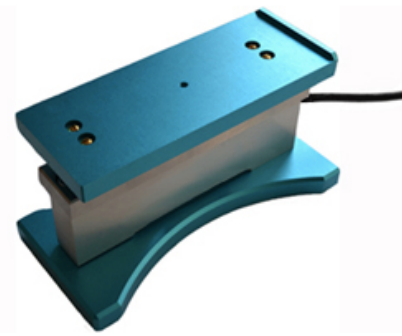


Figure 3.4: The FORCEBOARD utilized for friction measurement

3.4.1 Matlab friction measurement

The FORCEBOARD is equipped with an A/D converter and a strain gauge transducers that gives analog signal output from load in horizontal and vertical directions. A/D converter hardware is of the brand LABJACK and have compatible drivers for MATLAB. The program written in MATLAB is designed to measure the friction dependency due to wear, since measurements over long time is required. A flowchart of the program is displayed in Figure 3.5. The input for the FORCEBOARD is the vertical and horizontal force. The strain gauge transducers delivers analog signals proportional against the vertical and horizontal forces. The FORCEBOARD have five different channels but only channel four and five are used for these measuring purpose. From a streaming test the analog signals was sampled and stored, data are processed afterwards. Standard weights are used to calibrate the analog output to force. Before each test forces in vertical and horizontal direction are calibrated.

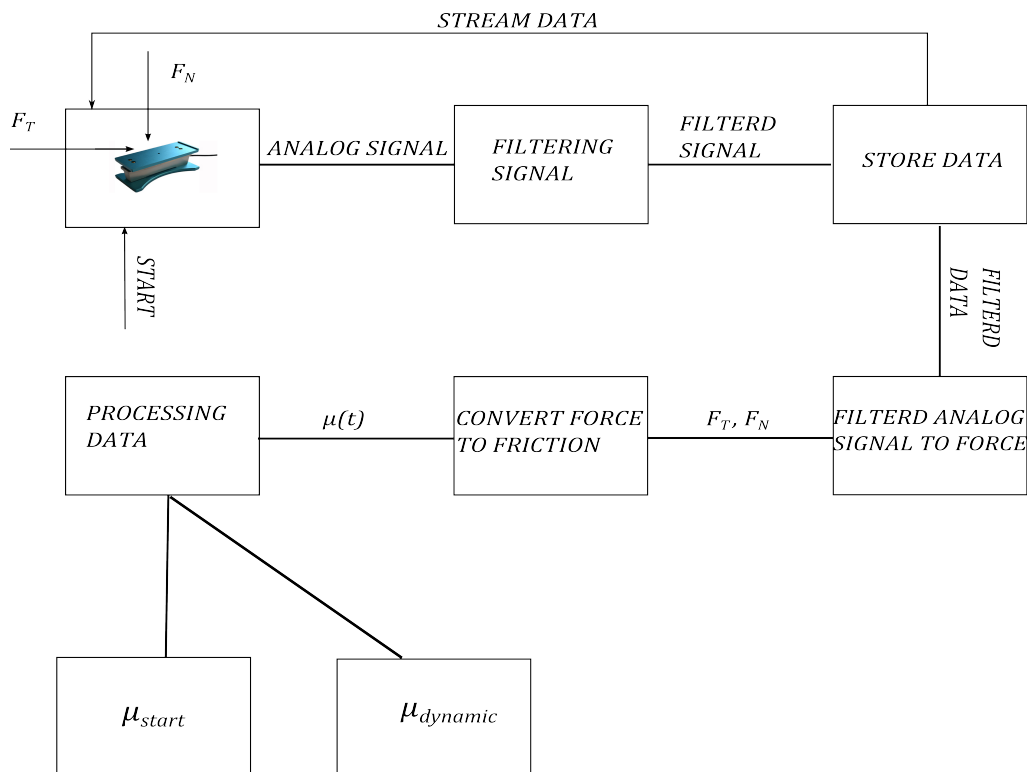


Figure 3.5: Flowchart of process from applied force to μ_{static} and $\mu_{dynamic}$

The measured signal contains a lot of noise and this behavior is eliminated by a second order lowpass Butterworth filter with a cut off frequency at 50 Hz. [13] Streamed test data from two different channels are sampled at a frequency at 10000 Hz, to avoid problems with lack of memory in the computer all raw data are saved after each minute to *.mat* files.

Collected data from an experimental session are stored and processed afterwards. The purpose of processing data is to obtain the static- and dynamic coefficient of friction. Common for all static friction points before transition to dynamic is high derivatives and function values at the quote in equation (2.17). From normalized value for derivatives and function values a generalized script for all tests are adapted. The dynamic friction is evaluated as the mean value of all samples during one second after the static friction occurred. To evaluate the results one static- and dynamic value are stored for each experimental cycle.

3.5 Test set up

In order to obtain a high repeatability of the experiments, a test rig is designed by help from test engineers at KONGSBERG AUTOMOTIVE. The test set up are displayed in Figure 3.6. The FORCEBOARD is fixed to a plate attached to a cart which can move in the horizontal direction. Movement of the rig is created by utilizing an air cylinder, where the air flow generates a force which causes the movement. The plunger is connected to the rig with a similar track as the lower cart and can only move in the vertical direction. To create a similar situation arising in the gear shifter an external load at 50 N is applied. Along with the own weight of the plunger connection the total load for the experiments is approximately 60 N.



(a) Test set up front view

(b) Test set up side view

Figure 3.6: Test set up utilized for measurements

One cycle involves a movement of 50 mm back and forth. The applied force in the horizontal direction is adjusted by the air inlet in the cylinder. Since the air inlet isn't symmetric in front and back, it was hard to find a settings of similar conditions in both directions. Therefore, only one direction is considered for evaluations. A cycle back and forth is set to six seconds to reduce generation of frictional heating in the tribological system. The air cylinder is controlled by giving the number of repeatable cycles. One minute of tests corresponds to ten values of static- and dynamic friction respectively. The mean values for each minute are utilized for the evaluation part.

3.6 Measurements

The experiments are divided into different subcategories, material- and surface texture tests. The material tests are made during different timescales and surface textures with various surface roughness, see Figure 3.7. Textured number two corresponds to the least rough surface while number three have the most rough surface. For all used samples in the material tests surface roughness R_a are presented in Table 3.2. Each R_a value refer to a specific texture as shown in Figure 3.7. Texture tests are performed with the same ABS resin material. The reason is that test plates was reference structures made by an injection molding toolmaker with no material options. The purpose of the material tests are to compare different materials against each other and see how the results correlates for the three different textures. Tests are also conducted with replacement of a steel sphere instead of the polymeric plunger to investigate affect of wear. The purpose is also to investigate if a steel plunger can replace a plunger made of polymer. All combinations of plungers and test plates for the material tests are presented in Figure 3.8.

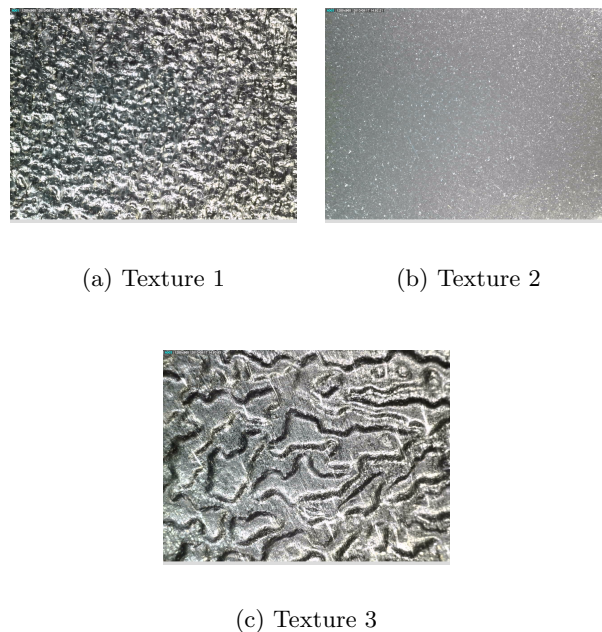


Figure 3.7: Surface texture of test plates at 50 times enlargement

Materials in tests

The materials used in tests are variations of POM and PA . The difference between POM alternatives are the additives which are chosen of the granule supplier. POM is as mentioned before a polymer with excellent tribological properties. Even though the molecular structure of the plunger (PA) and

test plates of PA-1 and PA-2 are a bit different it is interesting to see if any relation to the adhesion can be drawn. Some of the materials are produced in the purpose for friction measurement in this thesis and some were produced in the same injection molded tool since past.

POM Hostaform materials

The different POM combination utilized in the material test are presented below. Materials are denoted as POM-X where POM refers to the copolymer belongs to the POM family. The X refers to different additives and are suitable for different applications. The following POM variants for the material test is presented below:

- **POM-1** - Additive for good chemical resistance. Developed in purpose for low coefficient of friction and high resistance against wear.
- **POM-2** - Additives to reduce the coefficient of friction friction and prevent squeaking noise. Exhibiting good properties against chemical resistance and thermal degradation.
- **POM-3** - Additives with molybdenum disulfide and developed for applications with low sliding speed in combination with high contact pressures. Only show a small tendency to stick-slip phenomena, have good properties for resistance against thermal- and chemical degradation.
- **POM-4** - Developed for interiors in the automotive industry, exhibits high hardness and toughness. High crystalline thermoplastic with prize advantage.
- **POM-5** - Includes 20% of silicone developed for low coefficient of friction and high resistance against wear.

Polyamide materials

Two different test plates of polyamide are included in the material tests and one of them were reinforced with glass fiber. The molecular structure of the polyamides test plates are similar to the plunger of PA. The test plates of Polyamides are presented below:

- **PA-1** - Reinforced with 30% of glass fiber. Designed for high mechanical strength and can be used over a wide temperature range.
- **PA-2** - Possesses a fine combination of easy design and good mechanical strength. Suitable for use in a wide temperature range

Table 3.2: Material properties and R_a values of test plates

Material	E [MPa]	σ_y [MPa]	ε_y [%]	T_m [Celsius]	$R_{a,1}$	$R_{a,2}$	$R_{a,3}$
POM-1	2600	58	8	166	6.8	0.024	5.64
POM-2	2850	53	7	166	4.8	0.132	5.0
POM-3	2800	65	9	166	4.74	0.174	8.04
POM-4	2700	63	9	166	5.59	0.029	7.8
POM-5	2600	64	8	166	4.81	0.06	7.94
PA-1	7500	140	5	260	6.84	3.98	6.65
PA-2	1000	55	20	295	5.85	0.024	10.47

Material combination	30 minutes			60 minutes			900 minutes		
	Texture 1	Texture 2	Texture 3	Texture 1	Texture 2	Texture 3	Texture 1	Texture 2	Texture 3
PA/PA-1	X	X	X					X	
PA/PA-2	X	X	X					X	
PA/POM-1	X	X	X					X	
PA/POM-2	X	X	X					X	
PA/POM-3	X	X	X					X	
PA/POM-4	X	X	X					X	
PA/POM-5	X	X	X					X	
STEEL/PA-1					X				
STEEL/PA-2					X				
STEEL/POM-1					X				
STEEL/POM-2					X				
STEEL/POM-3					X				
STEEL/POM-4					X				
STEEL/POM-5					X				

Figure 3.8: Test matrix for the material test

30 Minutes tests

The 30 minutes tests are performed on seven in-house produced test plates with different surface textures, see Figure 3.7. These tests corresponds to 300 cycles. For all tests the plunger was made of PA material. The main purpose is to compare these combinations at initial stage before wear cause influence on the friction.

60 Minutes tests with steel

Test have been carried out for a steel plunger with polished surface against seven polymers. Tests are conducted for an hour which is equivalent to 600 cycles. Steel plunger geometry is identical to the polymeric plunger. All tests are performed at texture number two in Figure 3.7. The reason is that this texture is most similar to the surface of the actual application in the plunger track. Under these conditions, the polymer always is the softer material and therefore subjected to most deformation and wear. [9]

900 Minutes tests

The actual application shall be able to obtain a low friction over a lifetime which includes a high number of cycles (300000). This tests are necessary to evaluate the friction dependence of wear. The tests were run overnight and matched 9000 cycles. Tests are conducted on texture number two since the smoothness is most comparable to the plunger track, see Figure 3.7. A plunger made of PA were utilized for all tests and seven materials with surface texture number two represented the counter body.

3.6.1 Influence of contact pressure

The contact pressure is an important parameter for the friction and wear, see Section(2.6.6). To evaluate the influence of the contact pressure tests are performed with material POM-1 with different normal loads. Tests are performed on texture number two during one hour corresponding to 600 cycles. The plunger of PA is utilized for the tests and three different external loads are evaluated.

3.6.2 Texture tests

Tests are also conducted with 14 textures made of ABS resin with unknown material properties and a plunger made of PA. The reason is to evaluate how friction relates to surface topography. The textures are delivered by a toolmaker as mentioned before and these textures are references in their catalog. The different textures of the test plates is presented in Figure 6.1 to 6.4 in section Appendix 6.1. Data for for these textures, R_a and R_{max} values are presented in Table 3.3.

Table 3.3: R_a and R_{max} values of ABS resin with textures

Texture	R_a	$R_{max}[\mu m]$
Texture-1	0.64	3.77
Texture-2	8.13	40.3
Texture-3	1.73	11.0
Texture-4	2.61	16.3
Texture-5	6.5	27.3
Texture-6	6.07	39.6
Texture-7	9.31	47.7
Texture-8	1.21	8.88
Texture-9	1.46	8.14
Texture-10	1.26	8.45
Texture-11	2.21	15.0
Texture-12	1.72	9.71
Texture-13	2.25	15.2
Texture-14	1.77	10.6

4 Results

The simulation section compare different methods to evaluate stresses and deformation in the contact region and test section presents evaluated results from measurements.

4.1 Simulations

Generally the simulations yields a fairly good correlation against theoretical expressions. The plunger simulated as PA is subjected to the highest deformations and stresses due to the relative mechanical properties compared with POM as Table 3.1. The highest shear stress is located in the contact region for both two- and three dimensional models see Figure 4.1. Shear stress distribution from FEA shown in Figure 4.1a correlates well to simulation results from [7].

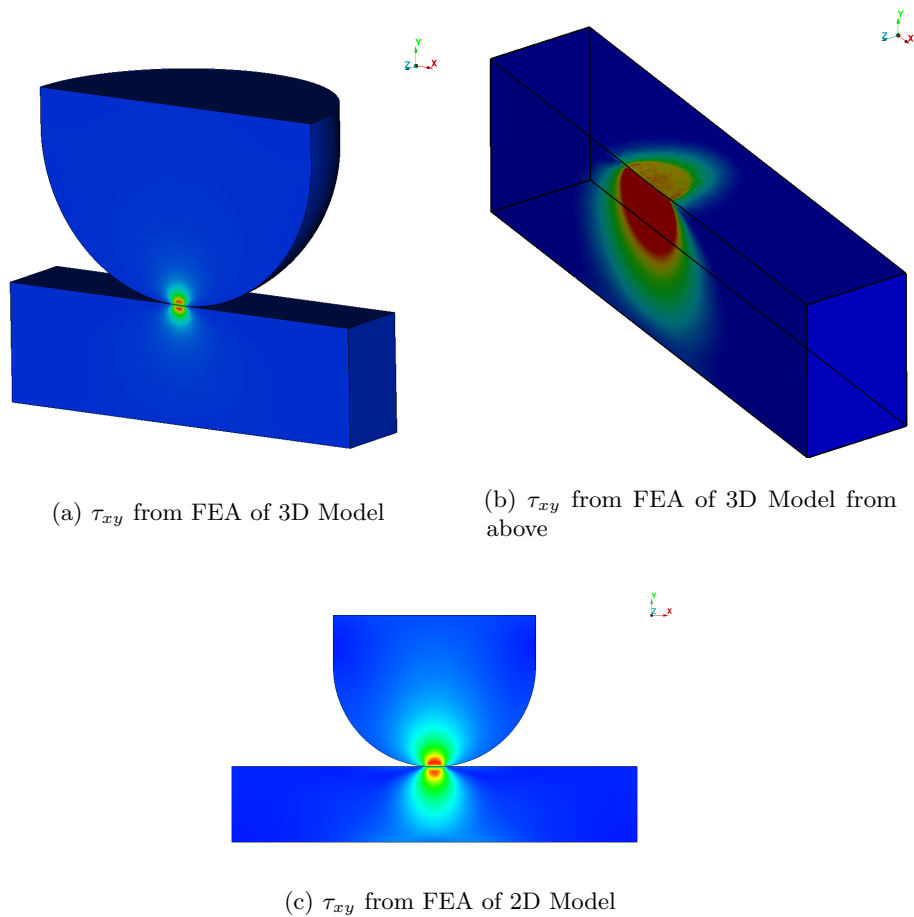
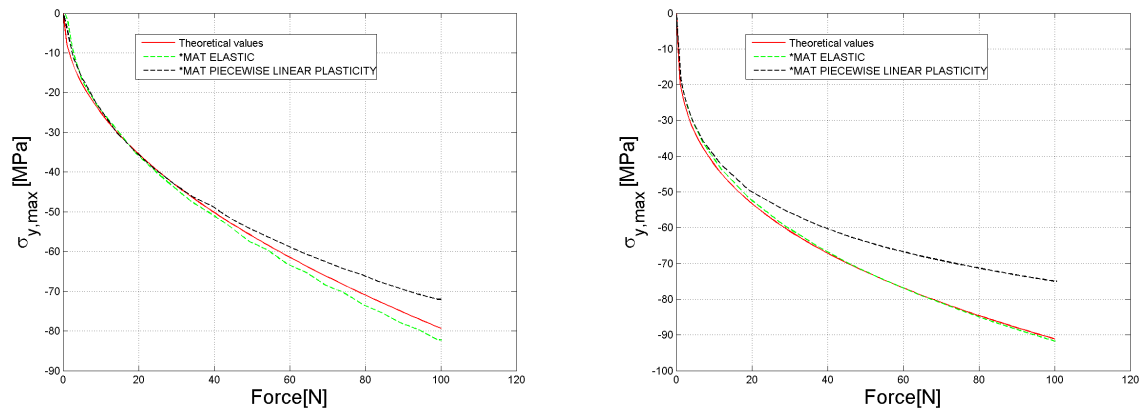


Figure 4.1: Shear stress distribution for different load case

Calculated normal stress for the three dimensional model correlate very well between theoretical values and elastic material properties implemented in the FE-model. When using the piecewise linear plasticity material model, the normal stress deviated from theoretical values for higher normal loads see Figure 4.2b. This is logical due to the plastic deformation in the contact spot. Similar behavior is obtained for the two dimensional model but the deviation with piecewise linear plasticity material properties were less compared to the three dimensional model as Figure 4.2a. For the case with elastic material models, almost perfect correlation with theoretical values are found.

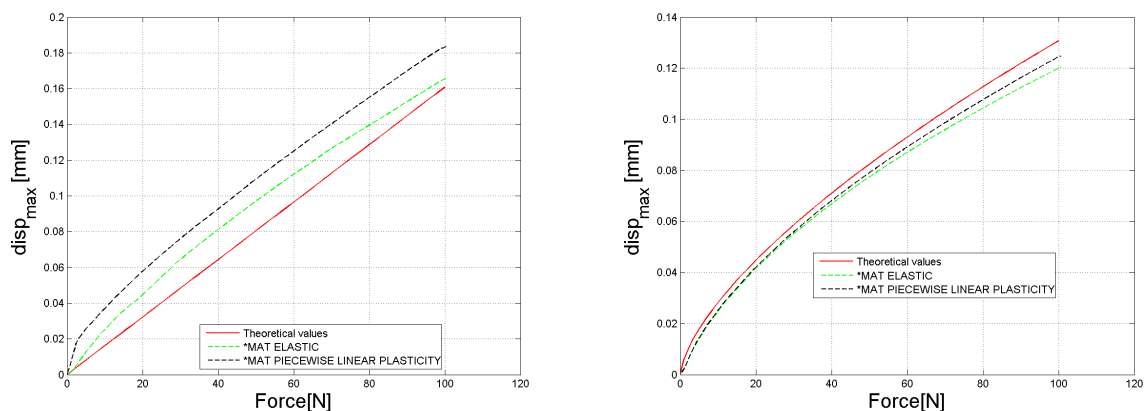


(a) σ_y from FEA and elastic theory for 2D model

(b) σ_y from FEA and elastic theory for 3D model

Figure 4.2: Normal stress for the 2D and 3D models

Comparisons for maximum displacement as function of force between elastic theory and finite element simulations yield a good correlation. For both 2D- and 3D the curve shapes are similar for all material models, but the correlation is better for the 3D case. Displacement for 2D- and 3D results are displayed in Figure 4.3a and 4.3b respectively. Difference for the 2D case is large in the beginning which might depend on the initial gap between plunger and plate in the FE-model. The reason may be explained in the contact formulations in LS-DYNA which are different for 2D- and 3D cases. Generally the deformation for the plastic material model is higher compared to pure elastic material properties which is logical.



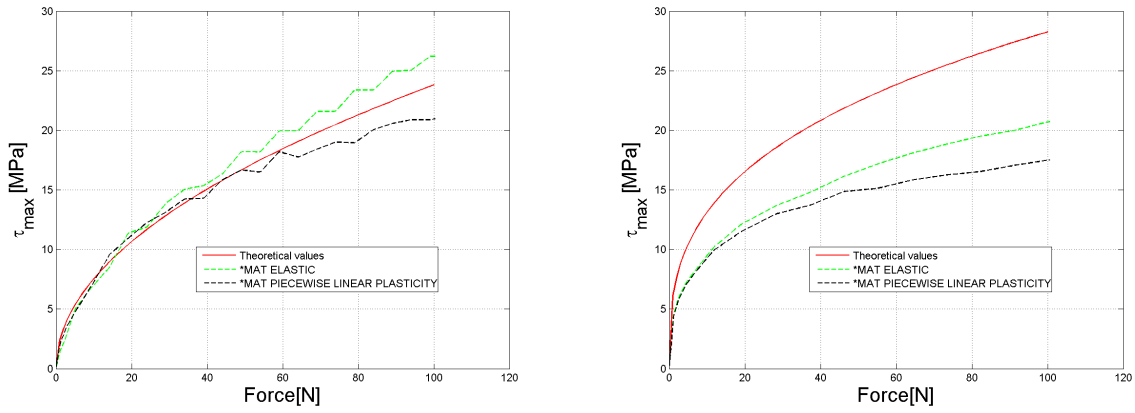
(a) Displacement from FEA and elastic theory for 2D model

(b) Displacement from FEA and elastic theory for 3D model

Figure 4.3: Displacement for the 2D and 3D models

Opposite to displacement the correlation for shear stress coincides better with theory for the 2D case, see Figure 4.4a. For the 3D case the deviations of the shear stress is large specially for the plastic material properties, see Figure 4.4b. The reason for the difficulty to predict the shear stress might be that the maximum shear stress moves within the structure for different loads. This behavior

is opposite to maximum normal stress and displacement which occurs in the same region for all loads.

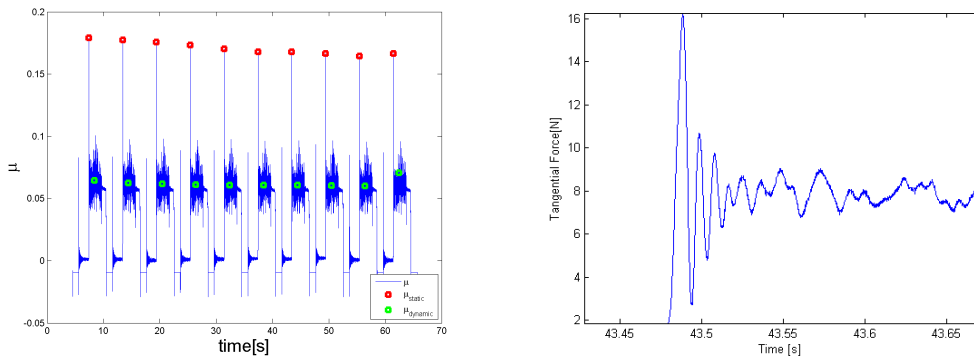


(a) τ_{xy} from FEA and elastic theory for 2D model (b) τ_{xy} from FEA and elastic theory for 3D model

Figure 4.4: Shear stress for the 2D and 3D models

4.2 Experimental results

The experiments are divided into different subcategories, depending on the timespan of the experiment and utilized texture. The main purpose is to compare the material against each other and evaluate the impact of different surface textures. The results are evaluated for each minute as discussed previously, each minute represent a mean value of the static- and dynamic coefficient of friction. One minute involves ten cycles back and forth, the static- and dynamic coefficient friction are displayed in Figure 4.5a. An example of the force curves during a test is displayed in Figure 4.6. The stick-slip phenomena discussed in Section 2.6.5 is observed for the tangential force during tests, see Figure 4.5b. Note that the transition from static- to dynamic friction occurs over a small time step, therefore a high sampling frequency is necessary for obtain this phenomena.



(a) Static and dynamic friction (b) Transition from static to dynamic friction

Figure 4.5: μ_{static} and $\mu_{dynamic}$ from test and stick-slip

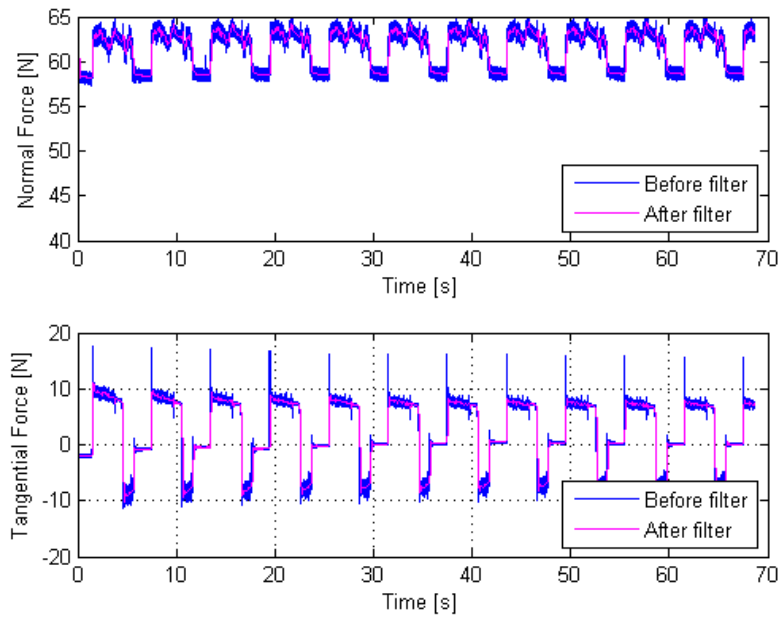


Figure 4.6: Normal and tangential force during one minutes test

4.2.1 Material 30 minutes tests

The 30 minutes tests are performed at the three different textures showed in Figure 3.7.

Texture 1 - 30 minutes test

The dynamic and static friction for texture one and seven different materials are presented in Figure 4.7. The time dependent coefficient of friction is presented in Table 4.1-4.2. Mean values for the coefficient of friction is listed in Table 4.3.

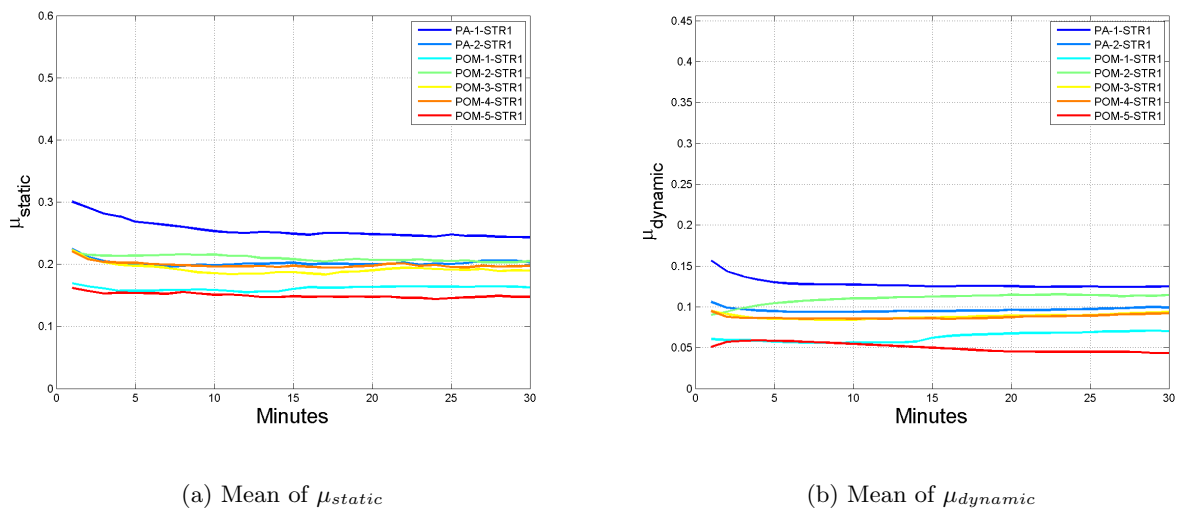


Figure 4.7: $\mu_{static}(t)$ and $\mu_{dynamic}(t)$ for the 30 minutes test, texture 1 and PA plunger

Table 4.1: μ_{static} for 30 minutes test at texture 1

Material	$t=1 \rightarrow 8$	$t=8 \rightarrow 16$	$t=16 \rightarrow 23$	$t=23 \rightarrow 30$
PA-1-STR1	0.275	0.251	0.247	0.244
PA-2-STR1	0.203	0.199	0.199	0.202
POM-1-STR1	0.159	0.157	0.162	0.163
POM-2-STR1	0.214	0.211	0.206	0.204
POM-3-STR1	0.201	0.185	0.188	0.190
POM-4-STR1	0.203	0.195	0.196	0.195
POM-5-STR1	0.154	0.149	0.146	0.145

Table 4.2: $\mu_{dynamic}$ for 30 minutes test at texture 1

Material	$t=1 \rightarrow 8$	$t=8 \rightarrow 16$	$t=16 \rightarrow 23$	$t=23 \rightarrow 30$
PA-1-STR1	0.135	0.126	0.125	0.124
PA-2-STR1	0.096	0.094	0.095	0.098
POM-1-STR1	0.057	0.057	0.066	0.069
POM-2-STR1	0.101	0.110	0.114	0.114
POM-3-STR1	0.087	0.085	0.088	0.091
POM-4-STR1	0.087	0.085	0.087	0.090
POM-5-STR1	0.056	0.052	0.046	0.044

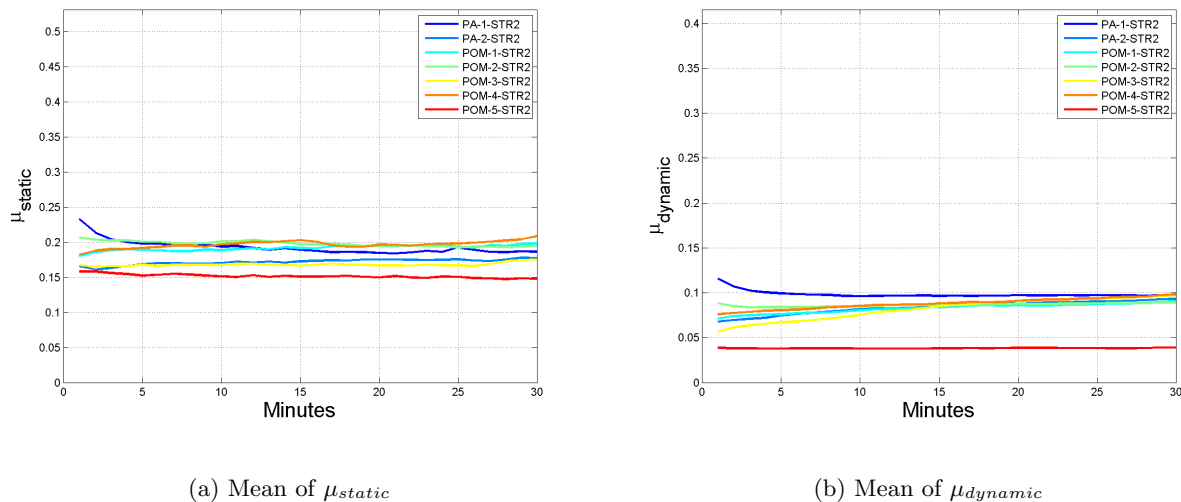
Table 4.3: Mean value of μ_{static} and $\mu_{dynamic}$ for 30 minutes test at texture 1

Material	$\mu_{mean,static}$	$\mu_{mean,dynamic}$
PA-1-STR1	0.254	0.128
PA-2-STR1	0.201	0.096
POM-1-STR1	0.160	0.062
POM-2-STR1	0.209	0.109
POM-3-STR1	0.191	0.088
POM-4-STR1	0.198	0.087
POM-5-STR1	0.149	0.050

Its clear from Figure 4.7 that static- and dynamic friction coefficient variations are small. The dynamic coefficient of friction is clearly less than the static, and follow the same pattern for all materials. All values for different materials are reasonably within the same span, but there are two materials (POM-1 and POM-5) which is significant lower compared with the higher (PA-1 with reinforced glass fiber). This is reasonable since PA-1 is a polymer that can withstand high mechanical loads while POM variants are designed for low friction applications. Although there are no drastic changes to any of the materials but there are some material combinations where coefficient of friction increases over time, while other showing an opposite behavior. However the differences are considered as very small between initial and final values.

Texture 2 - 30 minutes test

The static and dynamic friction for 30 minutes test at texture number two are displayed in Figure 4.8 and the time dependency are found in Table 4.4-4.5. Overall mean values for the static- and dynamic coefficient of friction is presented in Table 4.6.

Figure 4.8: $\mu_{static}(t)$ and $\mu_{dynamic}(t)$ for the 30 minutes test, texture 2 and PA plungerTable 4.4: μ_{static} for 30 minutes test at texture 2

Material	$t=1 \rightarrow 8$	$t=8 \rightarrow 16$	$t=16 \rightarrow 23$	$t=23 \rightarrow 30$
PA-1-STR2	0.204	0.191	0.185	0.186
PA-2-STR2	0.165	0.170	0.173	0.174
POM-1-STR2	0.186	0.189	0.193	0.194
POM-2-STR2	0.200	0.198	0.194	0.192
POM-3-STR2	0.165	0.167	0.166	0.168
POM-4-STR2	0.189	0.197	0.194	0.199
POM-5-STR2	0.154	0.151	0.149	0.148

Table 4.5: $\mu_{dynamic}$ for 30 minutes test at texture 2

Material	$t=1 \rightarrow 8$	$t=8 \rightarrow 16$	$t=16 \rightarrow 23$	$t=23 \rightarrow 30$
PA-1-STR1	0.135	0.126	0.125	0.124
PA-2-STR1	0.096	0.094	0.095	0.098
POM-1-STR1	0.057	0.057	0.066	0.069
POM-2-STR1	0.101	0.110	0.114	0.114
POM-3-STR1	0.087	0.085	0.088	0.091
POM-4-STR1	0.087	0.085	0.087	0.090
POM-5-STR1	0.056	0.052	0.046	0.044

Table 4.6: Mean value of μ_{static} and $\mu_{dynamic}$ for 30 minutes test at texture 2

Material	$\mu_{mean,static}$	$\mu_{mean,dynamic}$
PA-1-STR2	0.191	0.098
PA-2-STR2	0.170	0.083
POM-1-STR2	0.190	0.082
POM-2-STR2	0.196	0.086
POM-3-STR2	0.167	0.082
POM-4-STR2	0.195	0.088
POM-5-STR2	0.150	0.038

All materials are gathered in the same range concerning the coefficient of friction. Overall the tendency is that the mean coefficient of friction is less compared to texture one. Texture number two correspond to the finest surface according to Figure 3.7 despite this are static friction for POM-5 slightly higher compared to texture one. The dynamic coefficient for POM-5 is remarkable low, see Table 4.8. The trend is that POM-5 are clear less in both static and dynamic friction compared to all other materials. The deviation between the remaining materials is less compared texture one. As previous texture it's a clear difference between the static- and dynamic coefficient of friction where the dynamic is clearly less for all materials.

Texture 3 - 30 minutes test

As previously textures the static and dynamic coefficient of friction is depicted in Figure 4.9. The time dependency for coefficient of friction is presented in Table 4.7 and 4.8. Mean values for coefficient of friction is shown in Table 4.9.

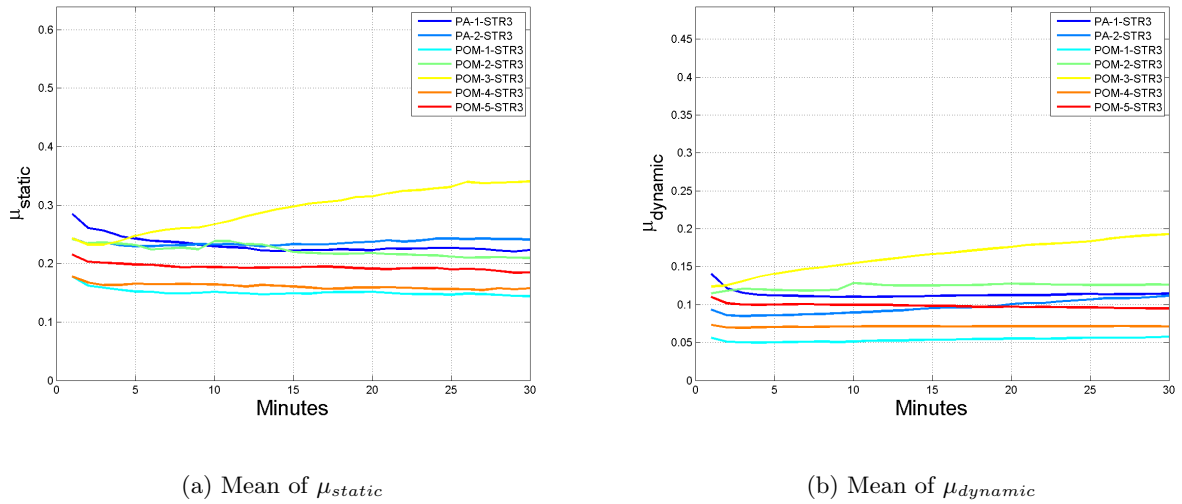


Figure 4.9: $\mu_{static}(t)$ and $\mu_{dynamic}(t)$ for the 30 minutes test, texture 3 and PA plunger

Table 4.7: μ_{static} for 30 minutes test at texture 3

Material	$t=1 \rightarrow 8$	$t=8 \rightarrow 16$	$t=16 \rightarrow 23$	$t=23 \rightarrow 30$
PA-1-STR3	0.249	0.225	0.223	0.223
PA-2-STR3	0.231	0.230	0.235	0.241
POM-1-STR3	0.155	0.148	0.148	0.145
POM-2-STR3	0.230	0.228	0.215	0.210
POM-3-STR3	0.244	0.279	0.313	0.333
POM-4-STR3	0.165	0.161	0.157	0.155
POM-5-STR3	0.199	0.192	0.191	0.188

The test for texture three follow the same pattern as texture one and two. They are generally low coefficient of frictions after 30 minutes except for POM-3 which increase linear over the 30 minutes. POM-1 obtained the lowest friction mean value over time. POM-5 are slightly higher compared to previous textures. Otherwise the POM-X materials show a similar pattern of the friction coefficient with some offset in values.

Table 4.8: $\mu_{dynamic}$ for 30 minutes test at texture 3

Material	$t=1 \rightarrow 8$	$t=8 \rightarrow 16$	$t=16 \rightarrow 23$	$t=23 \rightarrow 30$
PA-1-STR3	0.116	0.110	0.112	0.113
PA-2-STR3	0.087	0.091	0.099	0.107
POM-1-STR3	0.051	0.052	0.054	0.056
POM-2-STR3	0.118	0.124	0.126	0.126
POM-3-STR3	0.137	0.159	0.174	0.187
POM-4-STR3	0.070	0.071	0.071	0.071
POM-5-STR3	0.101	0.099	0.097	0.095

Table 4.9: Mean value of μ_{static} and $\mu_{dynamic}$ for 30 minutes test at texture 3

Material	$\mu_{mean,static}$	$\mu_{mean,dynamic}$
PA-1-STR3	0.230	0.113
PA-2-STR3	0.234	0.096
POM-1-STR3	0.149	0.053
POM-2-STR3	0.221	0.124
POM-3-STR3	0.292	0.164
POM-4-STR3	0.160	0.071
POM-5-STR3	0.193	0.098

4.2.2 Steel polymer test

Tests are performed with a spherical steel plunger with same diameter as the PA plunger. The tests was performed at texture two, see Figure 3.7. The static and dynamic coefficient for 60 minutes tests are displayed in Figure 4.10. Variation of the static- and dynamic friction coefficient for different time intervals are presented in Table 4.10 and 4.11. The mean value over 60 minutes are located in Table 4.12.

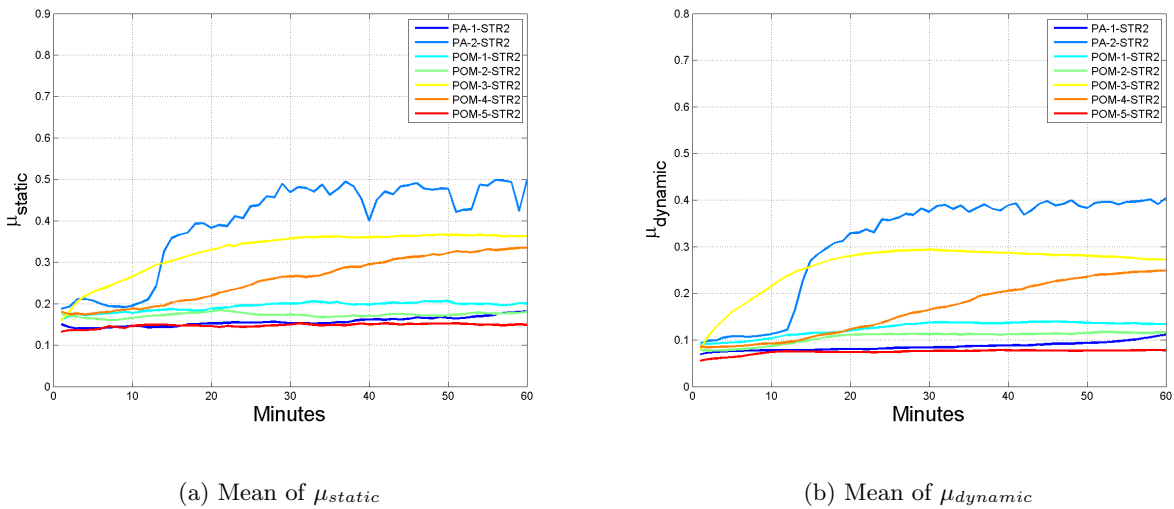
Figure 4.10: $\mu_{static}(t)$ and $\mu_{dynamic}(t)$ for the 60 minutes test, texture 2 and steel plunger

Table 4.10: μ_{static} for 60 minutes test at texture 2

Material	$t=1 \rightarrow 16$	$t=16 \rightarrow 31$	$t=31 \rightarrow 45$	$t=45 \rightarrow 60$
PA-1-STR2	0.143	0.152	0.156	0.169
PA-2-STR2	0.229	0.419	0.467	0.469
POM-1-STR2	0.176	0.191	0.200	0.199
POM-2-STR2	0.167	0.175	0.170	0.174
POM-3-STR2	0.248	0.337	0.359	0.362
POM-4-STR2	0.184	0.236	0.286	0.323
POM-5-STR2	0.142	0.145	0.149	0.149

Table 4.11: $\mu_{dynamic}$ for 60 minutes test at texture 2

Material	$t=1 \rightarrow 8$	$t=8 \rightarrow 16$	$t=16 \rightarrow 23$	$t=23 \rightarrow 30$
PA-1-STR1	0.135	0.126	0.125	0.124
PA-2-STR1	0.096	0.094	0.095	0.098
POM-1-STR1	0.057	0.057	0.066	0.069
POM-2-STR1	0.101	0.110	0.114	0.114
POM-3-STR1	0.087	0.085	0.088	0.091
POM-4-STR1	0.087	0.085	0.087	0.090
POM-5-STR1	0.056	0.052	0.046	0.044

Table 4.12: Mean value of μ_{static} and $\mu_{dynamic}$ for 60 minutes test at texture 2

Material	$\mu_{mean,static}$	$\mu_{mean,dynamic}$
PA-1-STR1	0.254	0.128
PA-2-STR1	0.201	0.096
POM-1-STR1	0.160	0.062
POM-2-STR1	0.209	0.109
POM-3-STR1	0.191	0.088
POM-4-STR1	0.198	0.087
POM-5-STR1	0.149	0.050

The results from the 60 minutes test with steel plunger showed more variation in results compared to 30 minutes tests. Initially all material started with both low static- and dynamic coefficient of friction. The most abrupt change could be seen for PA-2 which change dramatically after approximately 60 cycles. Subsequent increases the static coefficient of friction up to nearly 0.5 which is considered as very high. POM-3 show same pattern with low friction initially but also increase subsequent. The lowest coefficient of friction was obtained for POM-5 and PA-1. Values were slightly higher compared to 30 minutes test for the dynamic friction while the static was in the same range as the best obtained values in the 30 minutes tests. It's important to underline the good results obtained for combination of steel plunger and PA-1 compared to all textures in the 30 minutes tests.

4.2.3 900 minutes test

Compared to previous tests the 900 minutes clearly indicate the influence of wear. 900 minutes results in 9000 cycles and corresponds to a distance of 900 m, but this is significantly lower compared to repetition in a life-span for a gear shifter. In this tests both PA-1 and PA-2 was interrupted since they showed high wear and large increase in friction over time. Reason for interruption can be related to the limitations of test equipment according to Section 3.4. The static and dynamic friction for the 900 minutes test are displayed in Figure 4.11. Time dependent friction are presented in Table 4.13

and 4.14. Mean friction is presented in Table 4.15.

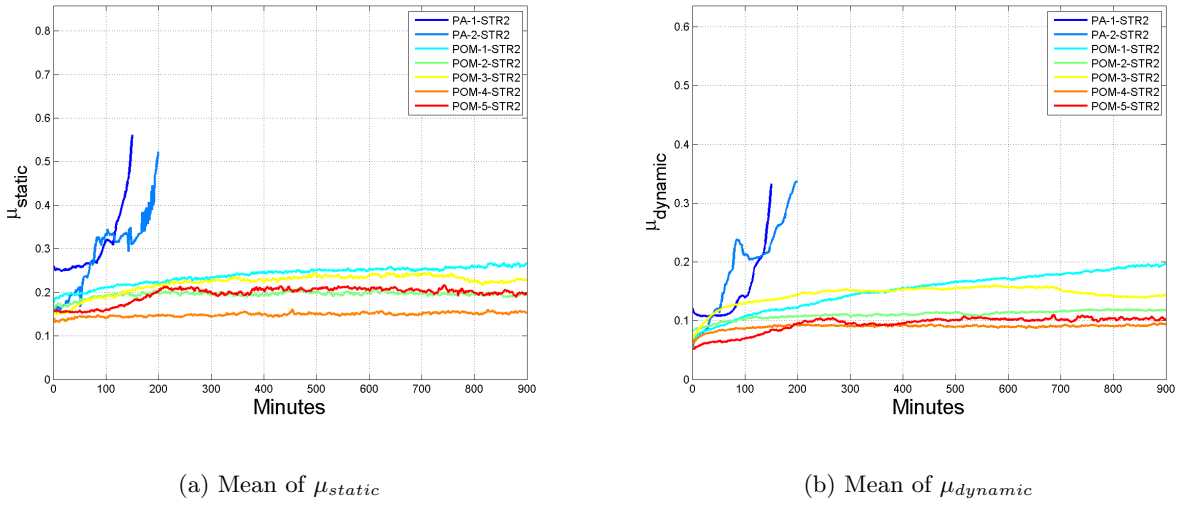


Figure 4.11: $\mu_{static}(t)$ and $\mu_{dynamic}(t)$ for the 900 minutes test, texture 2 and PA plunger

Table 4.13: μ_{static} for 900 minutes test at texture 2

Material	$t=1 \rightarrow 226$	$t=226 \rightarrow 451$	$t=451 \rightarrow 675$	$t=675 \rightarrow 900$
POM-1-STR2	0.20721	0.23751	0.2502	0.25617
POM-2-STR2	0.18794	0.19531	0.1982	0.19444
POM-3-STR2	0.1901	0.22583	0.23587	0.23039
POM-4-STR2	0.14256	0.14725	0.14992	0.15197
POM-5-STR2	0.15727	0.15771	0.1548	0.15465

Table 4.14: $\mu_{dynamic}$ for 900 minutes test at texture 2

Material	$t=1 \rightarrow 226$	$t=226 \rightarrow 451$	$t=451 \rightarrow 675$	$t=675 \rightarrow 900$
POM-1-STR2	0.10594	0.14651	0.16935	0.18682
POM-2-STR2	0.10108	0.10986	0.11285	0.11743
POM-3-STR2	0.12651	0.15138	0.15644	0.14506
POM-4-STR2	0.086115	0.091358	0.090188	0.091644
POM-5-STR2	0.052825	0.055387	0.057023	0.059089

Table 4.15: Mean value of μ_{static} and $\mu_{dynamic}$ for 900 minutes test at texture 2

Material	$\mu_{mean,static}$	$\mu_{mean,dynamic}$
POM-1-STR2	0.23774	0.15213
POM-2-STR2	0.19395	0.11029
POM-3-STR2	0.2205	0.14481
POM-4-STR2	0.14792	0.089822
POM-5-STR2	0.1555	0.0560

The 900 minutes test shows clearly the importance of wear for polymer tribo systems. Both PA-1 and PA-2 shows reasonable low static and dynamic friction coefficients in their initial phase but changed dramatically with increasing number of cycles. The static friction for PA-2 exhibits a very unstable behavior that probably depends on high wear. The different combination of POM shows a stable behavior over a large number of cycles. POM-5 which have shown good performance in previous test, tends to increase after 1200 cycles and then converge against a stable value. POM-4 obtain the best results over the 900 minutes as shown in Table 4.15. Except POM-4 all other POM variants show a slight increase of friction at the beginning and then stabilized. Remarkable is the increase of static friction coefficient for POM-1 it increase more rapidly than the static. After 9000 cycles the difference between the static- and dynamic friction is less compared to the initial deviation, see Table 4.13 and 4.14.

4.2.4 Friction dependence of normal load

The influence of the contact pressure and normal loads are also evaluated. External loads of two, four and six kilos was added except the self weight of the cart in vertical direction. The material for all experiments is POM-1 and texture two is considered on the test plates, see Figure 3.7. The static and dynamic friction are displayed in Figure 4.12. The time dependency of the friction are presented in Table 4.16 and 4.17. The overall mean results for the test are located in Table 4.18.

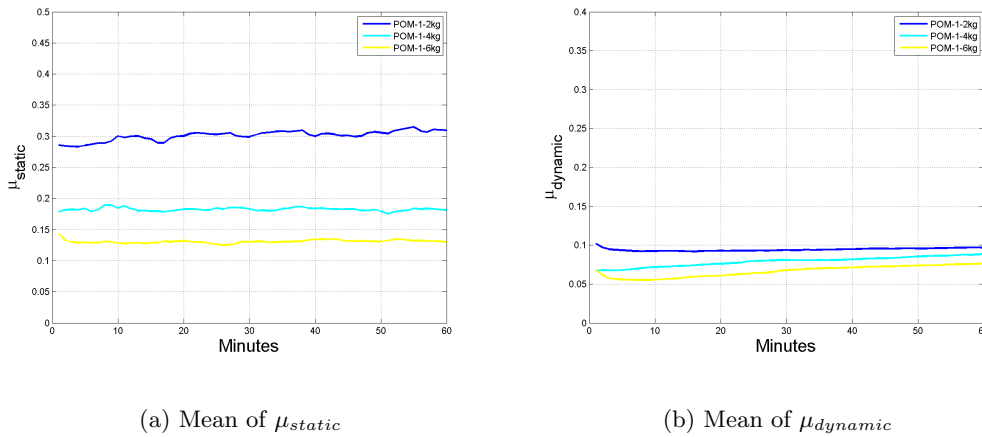


Figure 4.12: $\mu_{static}(t)$ and $\mu_{dynamic}(t)$ for the 60 minutes test, texture 2 and PA plunger

Table 4.16: μ_{static} for 60 minutes test at texture 2

Material	$t=0 \rightarrow 15$	$t=15 \rightarrow 30$	$t=30 \rightarrow 45$	$t=45 \rightarrow 60$
POM-1-2kg	0.093	0.092	0.094	0.096
POM-1-4kg	0.070	0.077	0.081	0.085
POM-1-6kg	0.057	0.062	0.070	0.074

Table 4.17: $\mu_{dynamic}$ for 60 minutes test at texture 2

Material	$t=0 \rightarrow 15$	$t=15 \rightarrow 30$	$t=30 \rightarrow 45$	$t=45 \rightarrow 60$
POM-1-2kg	0.287	0.296	0.300	0.304
POM-1-4kg	0.182	0.181	0.182	0.180
POM-1-6kg	0.129	0.128	0.131	0.131

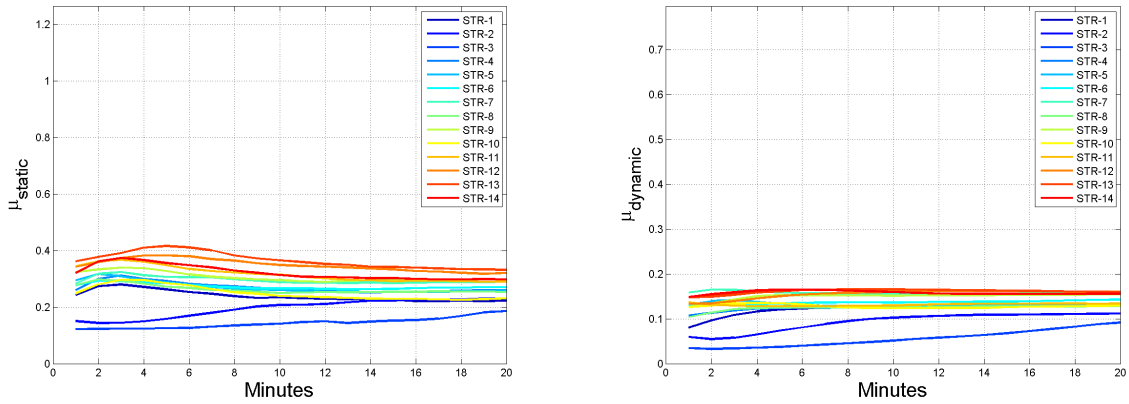
Table 4.18: Mean value of μ_{static} and $\mu_{dynamic}$ for 60 minutes test at texture 2

Material	$\mu_{mean,static}$	$\mu_{mean,dynamic}$
POM-1-2kg	0.297	0.094
POM-1-4kg	0.181	0.078
POM-1-6kg	0.130	0.066

It's proved that the coefficient of friction depends on the normal load. Opposite to the generalized trend in Section 2.6.6 a lower coefficient of friction is obtained for higher load for actual material combination. The difference in dynamic friction between different normal loads are greatest initially and then tend to go towards the same value after 600 cycles. The difference between the static friction is more stable during the 60 minutes. Notable is also that a low static friction is obtained at additional load of six kilograms equivalent to one kg more than the previously presented results. However, it is important to note that a higher normal force results in a greater tangential force to overcome motion, see Table 4.18. So mainly for the POM-1 in combination with PA plunger the coefficient of friction decrease with higher normal loads, however it's hard to generalize since the test only yield for three different loads.

4.2.5 Texture test

The dynamic and static friction for the 14 textures is presented in Figure 4.13. The x-label is limited to 100 minutes since further data is constant. The time dependent coefficient of friction is presented in Table 4.19-4.20. Mean value for the coefficient of friction is listed in Table 4.21.



(a) Mean of μ_{static} for each minute during 180 minutes tests

(b) Mean of $\mu_{dynamic}$ for each minute during 180 minutes tests

Figure 4.13: $\mu_{static}(t)$ and $\mu_{dynamic}(t)$ for the 180 minutes test at 14 textures and PA plunger

From results above its clear that the influence of texture significantly affect the coefficient of friction. At the initial stage a deviation in friction between the different textures are found. After approximately 50 cycles a tendency to either slightly bend up or down before convergence towards a stable value can be observed. Texture two and three yields the lowest initial static and dynamic coefficient of friction, the R_a , R_{max} and topography can be found in Table 3.2 and Figure 6.1. Except texture one and two the remaining textures are in same range for static and dynamic friction. In Figures 4.13 its clear that the static- and dynamic friction converge towards a stable value after approximately 30 minutes, this behavior can probably be explained by a stable wear rate is reached.

Table 4.19: μ_{static} for 180 minutes test at texture different textures

Texture	$\mu_{stat}t=1 \rightarrow 26$	$\mu_{stat}t=26 \rightarrow 51$	$\mu_{stat}t=51 \rightarrow 75$	$\mu_{stat}t=75 \rightarrow 100$
STR-1	0.12528	0.13602	0.14089	0.14401
STR-2	0.098115	0.12127	0.12858	0.1329
STR-3	0.066747	0.12492	0.13538	0.13985
STR-4	0.12703	0.13718	0.14203	0.14515
STR-5	0.13149	0.13881	0.14616	0.15051
STR-6	0.13859	0.15475	0.16546	0.17074
STR-7	0.15792	0.1668	0.17557	0.18154
STR-8	0.12551	0.13398	0.13921	0.14215
STR-9	0.15136	0.15976	0.16253	0.16511
STR-10	0.12879	0.14143	0.15153	0.15723
STR-11	0.13222	0.14424	0.15321	0.15823
STR-12	0.15614	0.16291	0.17093	0.17419
STR-13	0.16017	0.16018	0.16546	0.16872
STR-14	0.15782	0.16053	0.16583	0.16884

Table 4.20: $\mu_{dynamic}$ for 180 minutes test at texture different textures

Texture	$\mu_{dyn}t=1 \rightarrow 26$	$\mu_{dyn}t=26 \rightarrow 51$	$\mu_{dyn}t=51 \rightarrow 75$	$\mu_{dyn}t=75 \rightarrow 100$
STR-1	0.23389	0.21975	0.22369	0.22427
STR-2	0.20341	0.23952	0.25094	0.2549
STR-3	0.1576	0.23509	0.25113	0.26131
STR-4	0.26628	0.26528	0.2667	0.26807
STR-5	0.26665	0.26467	0.27419	0.28379
STR-6	0.27167	0.27824	0.28099	0.28582
STR-7	0.29369	0.30326	0.30803	0.31112
STR-8	0.26018	0.25749	0.25948	0.25917
STR-9	0.30374	0.2979	0.2972	0.29767
STR-10	0.24512	0.24178	0.25184	0.25807
STR-11	0.31104	0.29963	0.3046	0.30877
STR-12	0.34084	0.32255	0.33119	0.32985
STR-13	0.35669	0.32856	0.32998	0.32993
STR-14	0.317	0.30563	0.30685	0.30872

Table 4.21: Mean value of μ_{static} and $\mu_{dynamic}$ for 180 minutes test at texture different textures

Texture	$\mu_{mean,static}$	$\mu_{mean,dynamic}$
STR-1	0.2259	0.14214
STR-2	0.25067	0.12841
STR-3	0.24656	0.12899
STR-4	0.2689	0.14273
STR-5	0.28036	0.14824
STR-6	0.28573	0.16602
STR-7	0.31056	0.17925
STR-8	0.26099	0.14034
STR-9	0.297	0.16363
STR-10	0.25416	0.1521
STR-11	0.30615	0.1469
STR-12	0.33129	0.16599
STR-13	0.33661	0.16365
STR-14	0.3097	0.16323

4.3 Wear

From performed tests above the variation of friction over time is very clear. The reason is related to wear, which is difficult to measure and categorize. Some material combinations show a high wear on the surface while others exhibit a low wear despite a large number of cycles. This is perceived by microscopic observations. Transparent test plates made the evaluation of wear more complicated. Attempt to measure the depth of the track with the R_a -meter were carried out without any success of consistent results. The material exposed for high wear can easily be recognized, see Figure 4.14

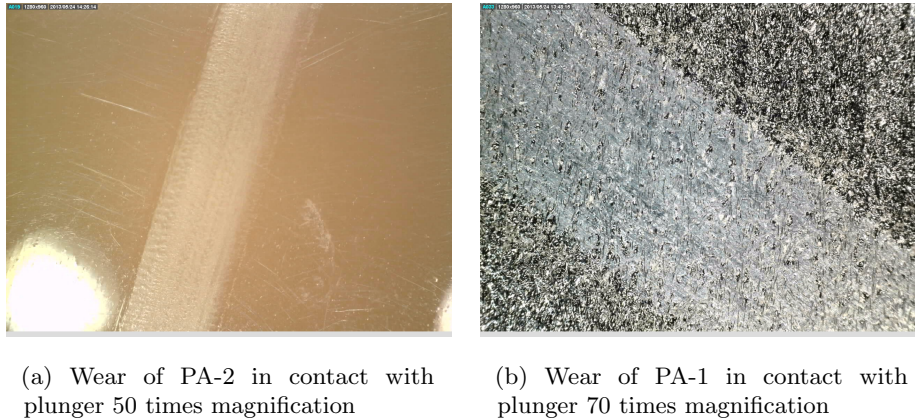


Figure 4.14: Wear of two polymers from tests

For the material tests the plunger of PA often act as the softer material see Table 3.1 and 3.2. Therefore it's important to examine the wear of the plunger. The relative material properties was important for the wear and for the longer test. The wear of the plunger seemed to be dependent on opposite material properties, glass fiber reinforcement and surface roughness. The wear of the plunger is significant for the case in contact with PA-1 which correspond to strongest material see Figure 4.15a. The debris on the surface is probably mainly from the plunger but also some PA-1 could be seen. For plunger against POM-3 the wear is clearly less see Figure 4.15b. Note that the material test for PA-1 was interrupted due to reason of high friction. Therefore the plunger in Figure 4.15b is exposed to a far larger number of cycles compared to plunger in Figure 4.15a.

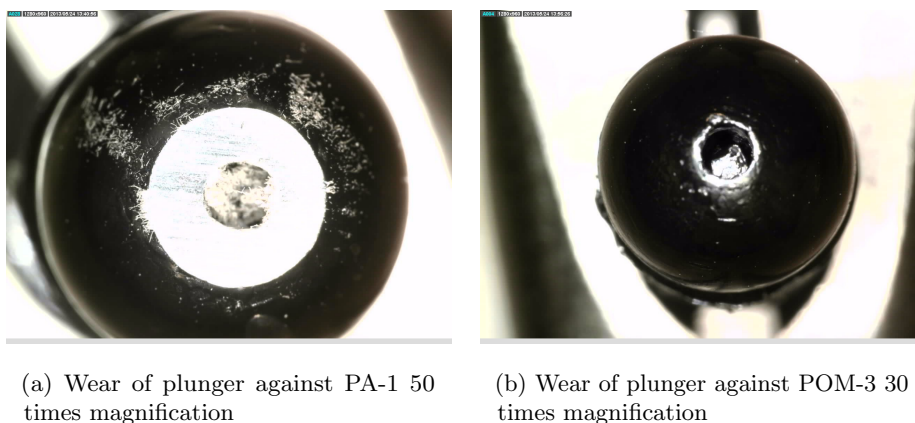


Figure 4.15: Wear of plungers from material tests

All the POM combination tolerate high load and large number of cycles without any significant wear. The wear of the 900 minutes tests can be seen in Section 6.2 and Figure 6.2. From the Figures its clear that wear of the test plates are very low. Test was conducted to measure the depth of the plunger trails. However it was hard to get any consistent result but the trails are in range of 0.1-0.3 mm. The wear of the POM variants are different, for example the hole of the plunger can be observed in 6.2b. The wear of PA-2 and PA-1 can be seen in Figure 4.14, note that those tests have not expired the 900 minutes. For the 60 minutes test with combination of steel-plunger the deformation zone was smaller for all materials see Figure 6.3 and 6.3. The only material that exhibit large wear was PA-2 which explain the increase in Figure 4.10. From the texture tests of the ABS resin is significantly that these test plates are softer than the plunger because all test plates exhibits a large wear after the 180 minutes test. The wear of the texture plates are located in Section 6.4 and presented in Figure 6.5 to 6.8. The wear explain the behavior the behavior of Figure 4.13, where there are some initial deviations in the coefficient of friction. Unfortunately the ABS resin was to poor to achieve a good investigation of the texture influence over time. The coefficient of friction converged against a stable value after a short time when the stable wear rate was reached as discussed in Section 2.6.8.

4.4 Summary of results

From a large number of performed test this section gives a brief summary of the results. Material tests have delivered blended results for different combinations of plunger and test plates. A summary of all material test can be seen in Figure 4.16. Overall have POM-5 shown good results in all test lengths and for both plunger alternatives. Generally all variants of POM has shown good results over all test lengths and plunger combinations besides a few exceptions where both the POM-3 and POM-4 showed a bad combination with the steel plunger. PA-2 have generally shown a bad results with combination of all plunger except for the shortest test with PA plunger. The glass fiber reinforced PA-1 have shown a poor combination with the plunger of PA but more stable coefficient of friction for the alternative with plunger of steel.

Material combination	30 minutes			60 minutes			900 minutes		
	Texture 1	Texture 2	Texture 3	Texture 1	Texture 2	Texture 3	Texture 1	Texture 2	Texture 3
PA/PA-1	Red	Yellow	Yellow					Black	
PA/PA-2	Yellow	Yellow	Yellow						
PA/POM-1	Green	Yellow	Green					Yellow	
PA/POM-2	Yellow	Yellow	Yellow					Yellow	
PA/POM-3	Yellow	Yellow	Red					Yellow	
PA/POM-4	Yellow	Yellow	Green					Green	
PA/POM-5	Green	Green	Yellow					Yellow	
STEEL/PA-1					Green				
STEEL/PA-2					Black				
STEEL/POM-1					Yellow				
STEEL/POM-2					Yellow				
STEEL/POM-3					Red				
STEEL/POM-4					Red				
STEEL/POM-5					Green				

	Catastrophic
	Poor
	Neutral
	Excellent

Figure 4.16: Outcome for the material test

Other tests have shown that the texture plays an important role in the friction and it is not obvious that the least rough surface provides the lowest friction. However, the material properties of ABS resin used in texture test proved to be inadequate, leading to a high wear. For the combination of PA plunger and test plate of POM-1 has shown that friction decreases with higher normal forces, although it is difficult to draw any conclusions with only three different load cases. The outcome of the wear has been mixed, it is possible to discern some trends where the plunger usually exposed to the highest wear except when it consists of steel. The reinforced PA-1 has a high tendency to tear the plunger. Any combination of POM provides a low wear on both the plunger and the test plates which is desirable and suitable for the gear shifter.

5 Conclusion and discussion

This section concludes this master thesis and suggestions for further work are also discussed. It also include some reflections of sustainable development related to the subject of this master thesis.

5.1 Conclusion

From experiment and literature its significant that tribological properties of material are hard to predict from simulations. The combination of materials is often more important than an individual material selection. Contact pressure due to applied load on current geometries is high and provides plastic deformation in the contact regions. This behavior has been observed despite the fact that the surfaces are modeled as ideally smooth. Although high contact stresses the various combinations of POM generally proved to be well suited for the application and maintained a stable level of both the static- and dynamic friction over a high number of cycles.

The FORCEBOARD has proved to be a great tool for measuring the coefficient of friction for different material combinations. However, a caution is taken to standardize obtained values in the friction tests. It is worth mentioning that the static friction is often significantly higher than the dynamic and it is unclear whether this is realistic or some phenomenon that occurs among force transmissions in the test rig. During this thesis, a dialogue has been conducted with a supplier of lubricants to KONGSBERG AUTOMOTIVE. They have partially used a FORCEBOARD to evaluate tests of various lubricants. In addition to the FORCEBOARD they also used more advanced test equipment to measure static and dynamic friction. Their conclusion was that the FORCEBOARD is a good tool to compare different options but the results should be considered with precaution when it comes to standardized coefficient of frictions.

The tests of 900 minutes are considered as the most reliable related to the actual application of the plunger against the plunger track in the gearbox shifter. These tests have clearly showed that a low friction at the initial state does not necessarily mean that it is a good combination of materials. Influence of wear on the plunger and test plates was found in these tests. For both PA-2 and PA-1 in combination with PA plunger the static coefficient of friction has increased more than 100 percent in less than 2000 cycles. Therefore it is very important to carry out a longer test where both coefficient of friction and wear are measured and analyzed before implementing materials in real applications.

Nevertheless no longer test was performed with the steel plunger it has shown a good performance for some material over the 600 cycles. Most notable is that the PA-1 showed very good performances together with the steel plunger compared to the PA plunger in other test. Therefore it might be possible to use more integrated plunger tracks in house materials if the combination of reinforced polymer and steel proves a good performance over the entire life-span. The explanation for the good performance of PA-1 and steel plunger can be related to the wear of the plunger. The wear was high against the PA plunger and almost absent for the steel plunger. These facts are in line with Section 2.6.9, which clarify that a combination of reinforced glass fiber polymers and steel is well suited for low friction and wear.

In general the coefficient of friction and wear was low for all POM variants. However it's hard to draw any conclusions of comparison with influence of lubrication since no further investigations is performed in this master thesis. It's important to mention that the additives played a significant role for both the friction and wear for the different POM variants. This work have omitted all dependency of velocity and temperature and this might be important to further investigate since the literature explained the importance of this. In general for polymer tribo systems it might be preferable to utilize different polymer types. From results it's observed that no combination of PA plunger and PA

test plates yield a good result. This can be referred to the importance of adhesion between polymers as treated in Section 2.6.4. The molecular bonds tend to increase in the contact region for similar materials and this behavior probably becomes more extensive for higher temperatures.

Its unclear why the normal force is not constant in time when the rig is pushed back and forth during tests. Figure 4.6 clearly shows that the normal force include a dynamic term. Explanation for this might be related to the deflection of the beam connected to the strain gauge transducer. Another possible reason might be related vibration refereed to the surface roughness of the test plates. However this dynamical contribution can't be considered as an obstacle to achieve good results since the FORCEBOARD measure the relation between forces instantaneous. The results from friction measurements proved to be more unstable for lower normal loads, therefore the normal load should preferable exceed 50 N for the FORCEBOARD. However a precaution must be taken to the limitation of the tangential force at 30 N for the device.

5.2 Sustainable development

Polymers are an excellent way of reducing the weight of vehicles by replacing metal parts with plastics. In turn this results in lower emissions and decrease the environmental impacts. But is this really the whole truth? It is irresponsible of engineers to believe that the environment should adapt to technical development when in reality its the opposite. During the development of new a product it is important to not only look at the applications lifetime without weighing in environmental aspects which goes beyond the products life-span. To reduce the impact on the environment a modern expression is green composites [3] which refers to materials that have as low impact on the environment as possible. When studying a product, its common to do a life cycle analysis that includes environmental impact from cradle to grave. Examples of what a life cycle analysis may contain are material and energy consumption in the manufacturing process. Recycling of composites are a natural way towards more sustainable development. However, there exist a lot of hidden issues behind this for example high disassembly costs. Its difficult for companies in competitive industries with low margins to solve environmental problems on their own. It might be good with various legislations to overcome the problems [3]. Thermoplastics are superior thermosets when it comes to recycling, however it is important to point out that a glass fiber-reinforced thermoplastic makes the recovery process much more difficult. A step in the right direction may be the introduction of natural fibers which refers to fibers that comes directly from nature e.g. fiber from different tree species [3]. However, it is a challenge to get materials reinforced by natural fibers as strong as glass fiber-reinforced materials. Implementation of natural fibers makes recycling of thermoplastics significantly simplified. Improvements and usage of sustainable materials will be a key issue in the future.

5.3 Further work

The test equipment must be evaluated by well-known material in terms of friction coefficients. Running a similar test with other test equipment can also be an alternative. There are several items of further interest in this thesis. Wear has a significant impact on coefficient of friction, therefore tests during longer time laps to further investigate the best material combination. These tests shall also involve different textures. All tests concerning friction and wear shall be tested in comparable number of cycles as the actual product to avoid undesirable problems. Issues with tests during this long time are that it will affect the time schedule for getting the product delivered. When many materials are possible candidates several test equipments are necessary for limit the time schedule. One option is to decrease the time of one cycle but then the frictional heat would increase in the tribo-system and that might play a crucial role for the outcome of tests. It is interesting to investigate more materials

with additives in purpose to get lower friction and wear. one additive that would be interesting to investigate is *polytetrafluoroethylene*(PTFE). It would be a good option to test material from other granules suppliers, as this thesis only focused on plastics from one supplier. Because this is also a mutual interest between buyer and supplier this might be some sort of cooperation. Results for different textures are also of great interest in such investigation but for certain requires a more representative materials compared to the ABS resin utilized in this master thesis.

The steel plunger showed low coefficient of friction and low wear for several tests. This is an interesting alternative which must be continued to investigate in the future. Using a steel plunger and replace the case with a glass fiber reinforced house and not using an external plunger track is cost saving. The plunger of PA has shown good results against the POM variants but showed higher wear against PA-1, therefore it is interesting to evaluate new option for plunger materials.

If there exists demand to go even deeper into the field of tribology a new test equipment might be necessary e.g. a commercial tribometer. This would give more standardized tests with more parameters such as temperature and velocity dependency. Wear can be investigated with a *Scanning electron microscope*(SEM) however this combination of equipment for friction and wear evaluation is very expensive.

Bibliography

- [1] Fischer-Cripps. A, C. *Introduction to contact mechanics - Second edition*. Springer, 2000.
- [2] Briscoe B, J. Tribology of polymers: State of an art. *Physicochemical Aspects of Polymer Surfaces*, 1:387–412, 1983.
- [3] Bastioli. C. *Green composites: polymer composites and the environment*. Woodhead Publishing Series in Composites Science and Engineering, 2004.
- [4] Delta-T Devices. *LS-DYNA KEYWORD USER'S MANUAL: Volume 2*, 2012.
- [5] Lancaster. J, K. Abrasive wear of polymers. *Wear*, 14:223–239, 1969.
- [6] Larsen-Basse J. Basic theory of solid friction. *ASM International*, 18:27–38, 1992.
- [7] Hoggmark-S. Jacobsson, S. *Tribologi - Friktion Smörjning Nötning*. Ångströmlaboratoriet, 2011.
- [8] Ludema. D Tabor K, C. The friction and visco-elastic properties of polymeric solids. *Wear*, 14:329–348, 1966.
- [9] Sinha. J B Briscoe. K, S. *Polymer Tribology*. Imperial College Press, 2009.
- [10] Kubat J. Klason, C. *Plaster: Materialval och materialdata*. Liber, 2008.
- [11] Nielsen. L, E. *Mechanical Properties of Polymers*. Reinhold publishing corporation, 1967.
- [12] Meyers. K K Chawla. M, A. *Mechanical behavior of materials*. Prentice Hall, 1999.
- [13] Matlab. *Matlab Manual version 8.0 (R2012b)-Signal processing toolbox*.
- [14] McCrum. C P Buckley. C B Bucknall. N, G. *Principles of Polymer Engineering - Second edition*. Oxford Science publication, 1997.
- [15] Harders H. Baeker M. Roesler, J. *Mechanical Behaviour of Engineering Materials*. Springer-Verlag Berlin Heidelberg, 2007.
- [16] Zhang S, W. State-of-the-art of polymer tribology. *Tribology International*, 31:49–60, 1998.
- [17] M Raob. P Liaob. Y K Chenc. S N Kukurekaa., C J Hookeb. The effect of fibre reinforcement on the friction and wear of polyamide 66 under dry rolling sliding contact. *Wear*, 190: Issue 2:107–116, 1999.
- [18] Popolov. V, L. *Contact Mechanics and Friction - Physical Principles and Applications*. Springer-Verlag: Berlin, Heidelberg, 2010.

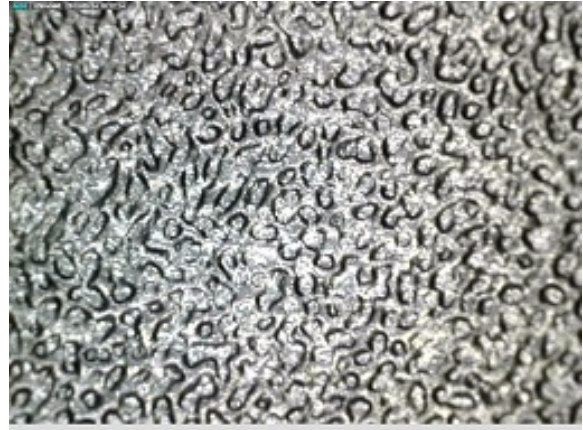
6 Appendix

6.1 Appendix A

6.1.1 Texture figures



(a) Texture 1



(b) Texture 2

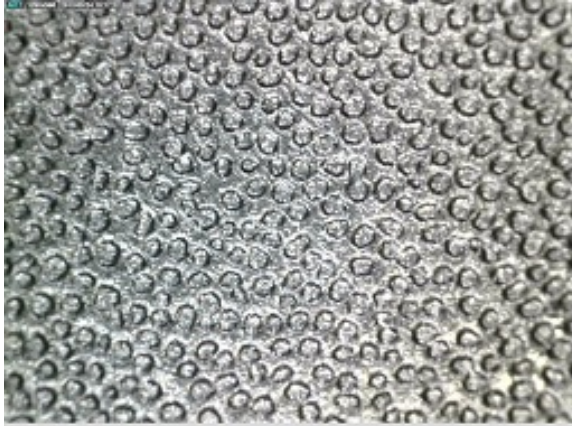


(c) Texture 3

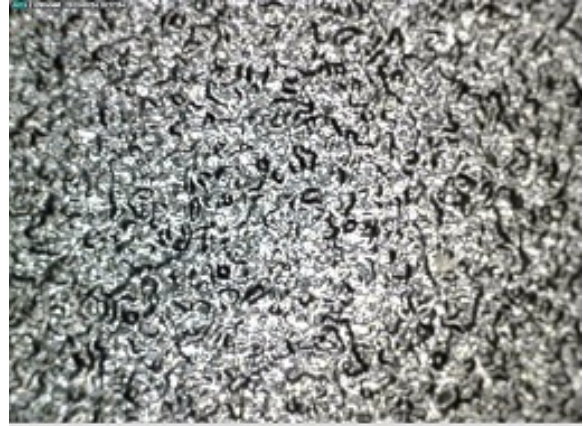


(d) Texture 4

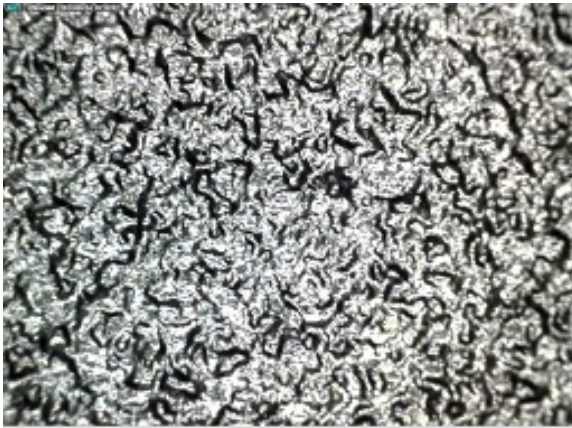
Figure 6.1: Surface textures at 50 times magnification



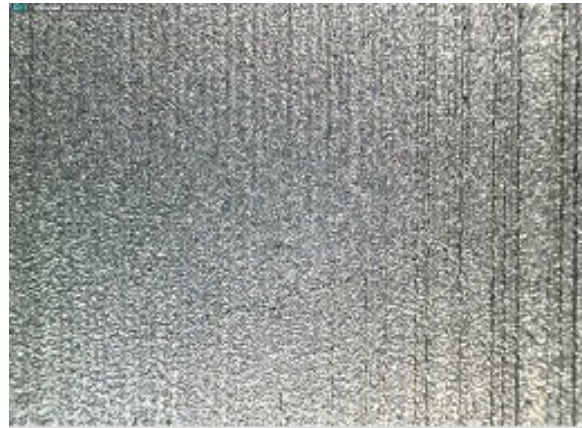
(a) Texture 5



(b) Texture 6

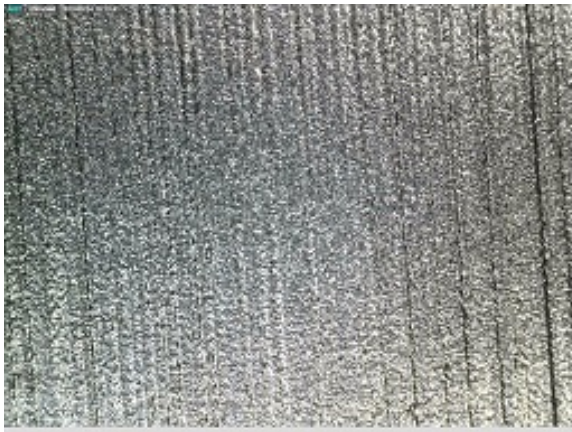


(c) Texture 7

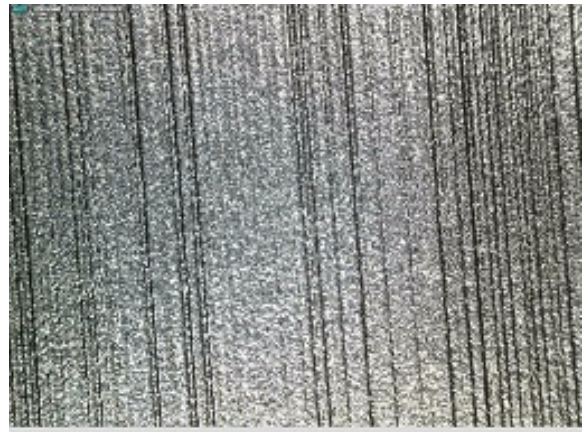


(d) Texture 8

Figure 6.2: Surface textures at 50 times magnification



(a) Texture 9



(b) Texture 10



(c) Texture 11



(d) Texture 12

Figure 6.3: Surface textures at 50 times magnification



(a) Texture 13

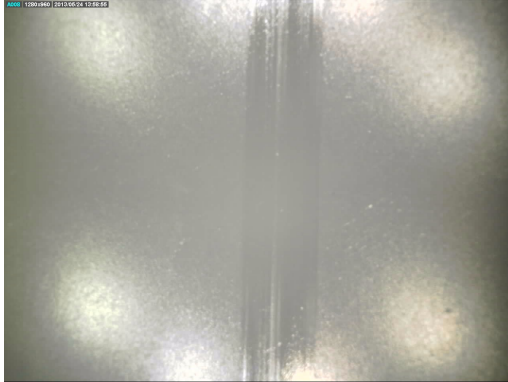


(b) Texture 14

Figure 6.4: Surface textures at 50 times magnification

6.2 Appendix B

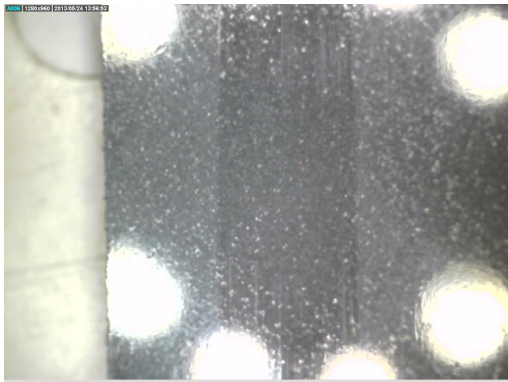
Deformation of the POM variants from the 900 minutes tests



(a) Deformed test plate of POM-1



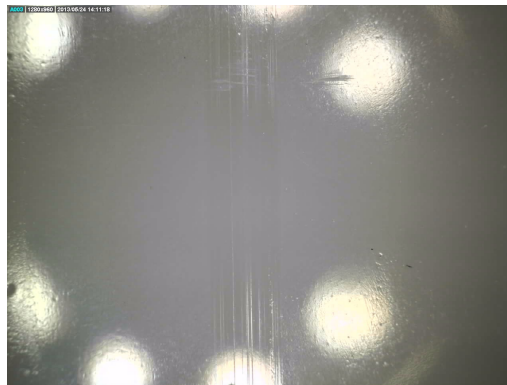
(b) Deformed test plate of POM-2



(c) Deformed test plate of POM-3



(d) Deformed test plate of POM-4



(e) Deformed test plate of POM-5

6.3 Appendix C

Deformation of the POM variants from the 60 minutes tests with steel plunger



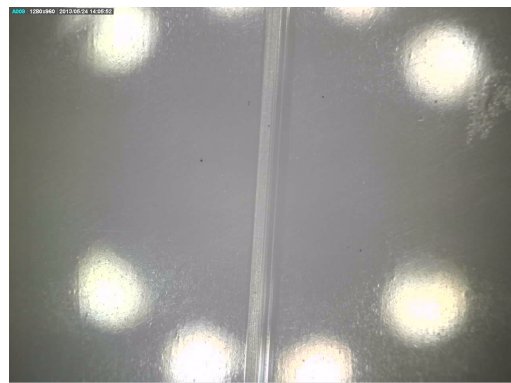
(f) Deformed test plate of POM-1



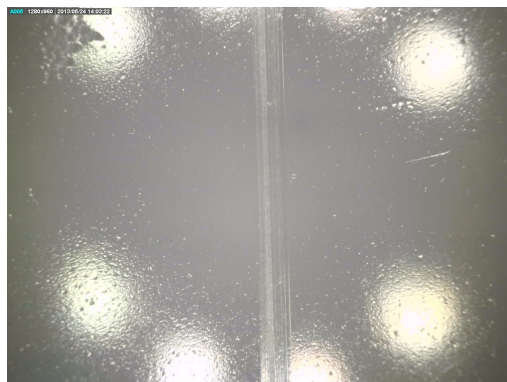
(g) Deformed test plate of POM-2



(h) Deformed test plate of POM-3



(i) Deformed test plate of POM-4



(j) Deformed test plate of POM-5



(k) Deformed test plate of PA-1



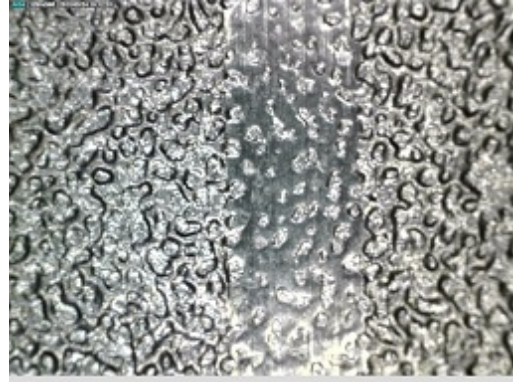
(l) Deformed test plate of PA-2

6.4 Appendix D

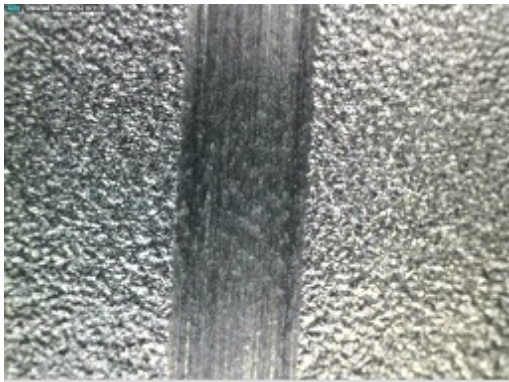
6.4.1 Texture figures



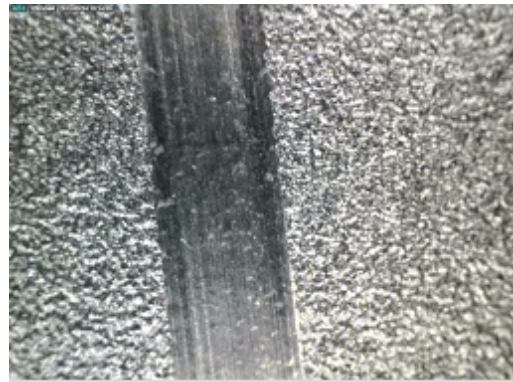
(m) Texture 1 deformed



(n) Texture 2 deformed

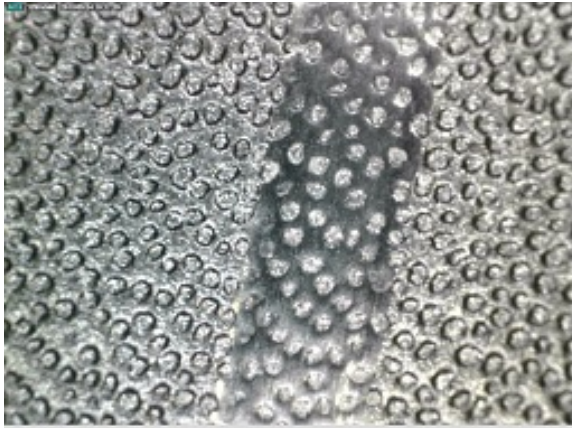


(o) Texture 3 deformed



(p) Texture 4 deformed

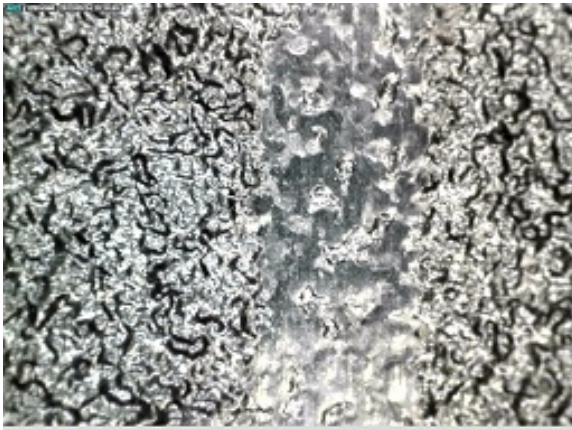
Figure 6.5: Surface textures at 50 times magnification after conducted test



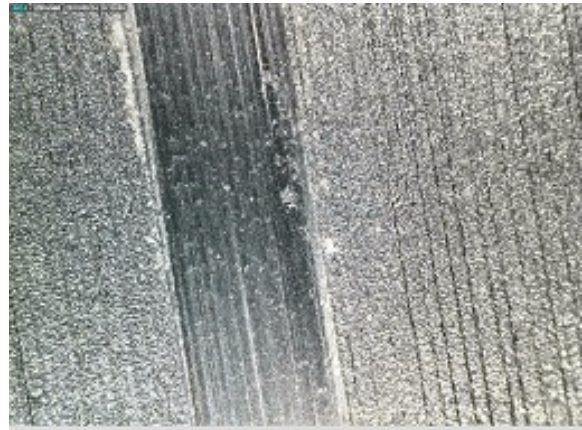
(a) Texture 5 deformed



(b) Texture 6 deformed

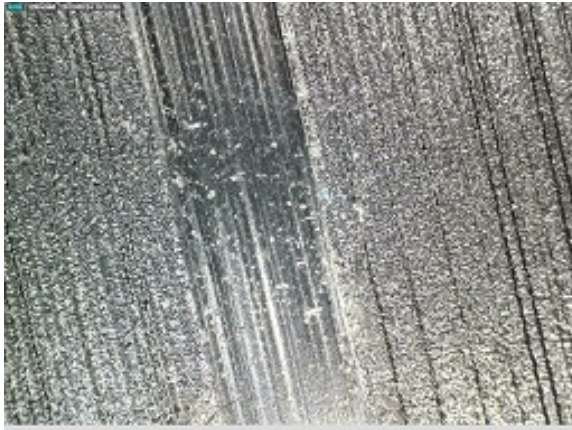


(c) Texture 7 deformed



(d) Texture 8 deformed

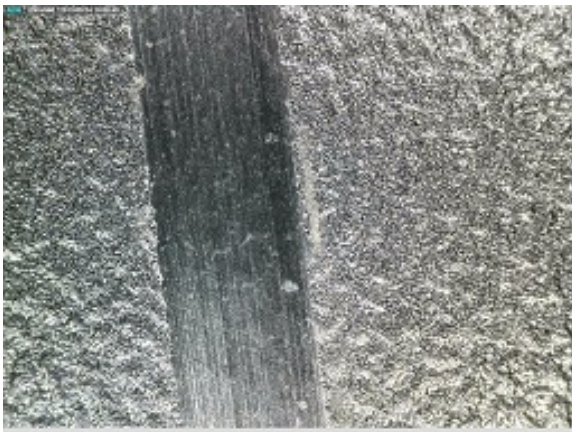
Figure 6.6: Surface textures at 50 times magnification after conducted test



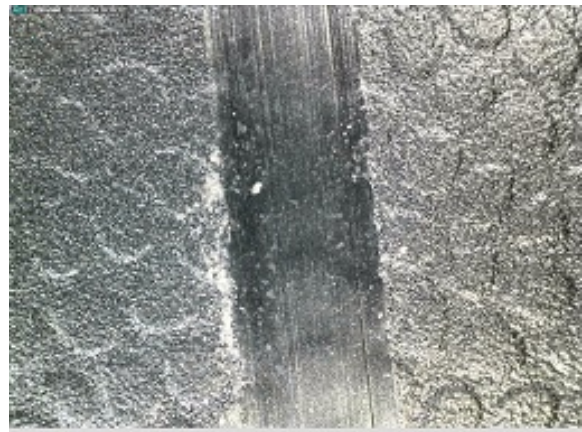
(a) Texture 9 deformed



(b) Texture 10 deformed



(c) Texture 11 deformed

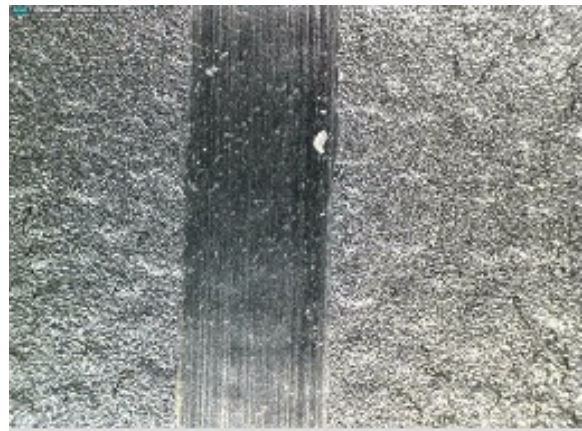


(d) Texture 12 deformed

Figure 6.7: Surface textures at 50 times magnification after conducted test



(a) Texture 13 deformed



(b) Texture 14 deformed

Figure 6.8: Surface textures at 50 times magnification after conducted test